NATIONAL ADVISORY COMMITTEE FOR AERONAUTICS

REPORT 1100

ON REFLECTION OF SHOCK WAVES FROM BOUNDARY LAYERS

By H. W. LIEPMANN, A. ROSHKO
and S. DHAWAN

1952

For sale by the Superintendent of Documents, U. S. Government Printing Office, Washington 25, D. C. Yearly subscription, $9.75; foreign, $11.00; single copy price varies according to size - - - - - - - - Price 30 cents

REPORT 1100

ON REFLECTION OF SHOCK WAVES FROM BOUNDARY LAYERS

By H. W. LIEPMANN, A. ROSHKO
and S. DHAWAN

California Institute of Technology

National Advisory Committee for Aeronautics

Headquarters, 1724 F Street NW, Washington 25, D. C.

Created by act of Congress approved March 3, 1915, for the supervision and direction of the scientific study of the problems of flight (U. S. Code, title 50, sec. 151). Its membership was increased from 12 to 15 by act approved March 2, 1929, and to 17 by act approved May 25, 1948. The members are appointed by the President, and serve as such without compensation.

Conduct, under unified control, for all agencies, of scientific research on the fundamental problems of flight

REPORT 1100

ON REFLECTION OF SHOCK WAVES FROM BOUNDARY LAYERS [1]

By H. W. Liepmann, A. Roshko, and S. Dhawan

SUMMARY

Measurements of the reflection characteristics of shock waves from a flat surface with a laminar and turbulent boundary layer are presented. The investigations were carried out at Mach numbers from about 1.3 to 1.5 and a Reynolds number of 0.9×10^6.

The difference in the shock-wave interaction with laminar and turbulent boundary layers, first found in transonic flow, is confirmed and investigated in detail for supersonic flow. The relative upstream influence of a shock wave impinging on a given boundary layer has been measured for both laminar and turbulent layers. The upstream influence of a shock wave in the laminar layer is found to be of the order of 50 boundary-layer thicknesses as compared with about 5 in the turbulent case. Separation almost always occurs in the laminar boundary layer. The separation is restricted to a region of finite extent upstream of the shock wave. In the turbulent case no separation was found. A model of the flow near the point of impingement of the shock wave on the boundary layer is given for both cases. The difference between impulse-type and step-type shock waves is discussed and their interactions with the boundary layer are compared.

Some general considerations on the experimental production of shock waves from wedges and cones are presented, as well as a discussion of boundary layer in supersonic flow. A few examples of reflection of shock waves from supersonic shear layers are also presented.

INTRODUCTION

The investigations on the reflection of shock waves from boundary layers reported here form part of an experimental study of viscous effects in high-speed flow. Experimental results of the last 10 years have shown that viscous effects in supersonic and especially in transonic flow are often very important and quite different from comparative results in subsonic flow. The earliest results of this nature are due to Ferri (reference 1) who observed separation of the boundary layer from the rearward part of a supersonic airfoil section in a region of expected favorable pressure gradient. A little later Donaldson (reference 2) discussed briefly the strong boundary-layer influence upon the shock wave in a duct. The apparent disagreement between theory and experiment in transonic flow and also among various experimental results prompted a thorough investigation of boundary-layer effects in transonic flow. Investigations of this nature were started independently by Ackeret, Feldmann, and Rott (reference 3) in Switzerland and by groups at the National Advisory Committee for Aeronautics (reference 4) and at the Guggenheim Aeronautical Laboratory, California Institute of Technology (reference 5), in this country. The results of all these investigations showed a rather startling influence of the boundary layer upon the whole flow field.

The detailed measurements at GALCIT and especially those by Ackeret, Feldmann, and Rott showed a number of interesting interactive effects between shock waves and boundary layer. The measurements in transonic flow were very important in showing up the strong boundary-layer effects and also in cautioning comparisons between experiment and inviscid theory in transonic flow. However, the complication of the transonic-flow problem made an analytical evaluation of the results, and specifically of the boundary-layer influence, impossible. It was therefore necessary to attempt to simplify the interaction problem as much as possible without losing any important features. To do this a general qualitative analytical study of the general problem of viscous effects in high-speed flow was necessary, coupled with a careful experimental investigation of the important viscous effects in transonic and supersonic flow (reference 6). Experiments and simple theoretical consideration showed that in transonic and supersonic flow there exist viscous (and turbulent) effects which are of a different nature and often of a different order of magnitude from comparable phenomena in subsonic flow. Various phenomena of this type have been qualitatively discussed in references 6 and 7. Speaking in broad and loose terms, the difference in viscous effects in supersonic as compared with subsonic flow is due to the fact that the outer flow field is hyperbolic and therefore rather sensitive to local changes in the boundary conditions and that the interaction between the outer supersonic field and the necessarily subsonic field existing near solid surfaces is quite different from the interaction in purely subsonic flow. Viscosity makes purely supersonic flow past solid boundaries impossible whenever the no-slip condition is satisfied.

Except for an extension of standard boundary-layer theory to high-speed flow there hardly existed any theoretical approach to viscosity effects in supersonic flow. A consideration of the well-known Pohlhausen method with simple supersonic-flow theory has been used in attempts to compute interactive effects between boundary layers and supersonic flow. (See references 6, 8, and 9.) Recently Lagerstrom and his coworkers have started a broad theoretical investigation of viscous, compressible flow (reference 10). The excessive mathematical difficulties of dealing with the full nonlinear equations made simplifying assumptions imperative and, therefore, so far, a direct comparison between measure-

[1] Supersedes NACA TN 2334, "On Reflection of Shock Waves from Boundary Layers" by H. W. Liepmann, A. Roshko, and S. Dhawan, 1951.

ments and theory is not possible. But there is now some hope that the gap can be narrowed in the not too distant future; at least qualitative agreement in a few cases has been established.

The problem of the reflection of oblique shock waves from a flat surface with a boundary layer appeared to be the simplest case to be investigated experimentally and the results of measurements of this type are here reported.[2] It was intended to study first, before proceeding to the boundary-layer problem, the reflection and transmission of shock waves through supersonic shear layers, that is, parallel layers in which the velocity and Mach number change at constant pressure but nowhere become subsonic. For such shear layers and weak shock waves a theory has been given by Marble (reference 12), and a comparison appeared useful. The production of simple stable shear layers, however, proved very difficult indeed and only a few measurements were made.

During the attempts to set up clean experimental conditions both for a shear layer and for a boundary-layer interaction, it was found necessary to investigate the distribution of pressure and general nature of the shock waves which were used in the interaction process. This study led to some interesting and, in many respects, rather surprising results which are discussed in the section "Remarks on Shock Waves" of this report.

One may ask here why a complicated phenomenon such as the interaction between shock waves and boundary layer is investigated before the boundary layer in a uniform supersonic flow has been studied carefully. The reason for this apparently illogical approach is that the problem grew naturally from the earlier investigations of transonic flow. The interaction between shock waves and boundary layer makes the flow problem complicated but the resulting effects are very large and comparatively easy to measure. To study detailed boundary-layer flow alone, small and slowly varying parameters have to be measured. It is hoped that the instrumentation developed in the investigation of shock-wave and boundary-layer interaction can be further refined and used in investigating boundary layers in uniform flow.

The present investigation was carried out at GALCIT under the sponsorship and with the financial assistance of the National Advisory Committee for Aeronautics. The authors wish to acknowledge the cooperation of Messrs. Harry Ashkenas and Raymond Chuan; discussions with Drs. Lagerstrom and Cole were of great assistance.

SYMBOLS

b	thickness of subsonic region (reference 13)
d	distance, along flow direction, from leading edge of plate
H_1	height of region of influence of disturbance depending on angle of wedge sides
H_2	height of region of influence of disturbance depending on nose bluntness
k	reflection coefficient (reference 14)
M	local Mach number
M_1	Mach number of uniform flow ahead of shock-wave system; also Mach number in supersonic stream (reference 14)
M_2	Mach number of uniform flow behind shock wave; also Mach number in subsonic stream (reference 14)
M_3	Mach number behind various shock configurations
$\overline{M}$	mean Mach number
p	local static pressure
p_1	static pressure of uniform flow ahead of shock wave
p_2	static pressure of uniform flow behind shock wave
p_3, p_4	static pressures behind various shock configurations
p_o	reservoir stagnation pressure or total head
p_o'	local total head
p_s	static pressure on surface of cone
p_w	static pressure just after initial pressure jump through conical shock wave
R	Reynolds number at point of measurement on surface of plate ($U_1 d\rho_1/\mu_1$)
t	shock-wave thickness
U	velocity in boundary layer
U_1	velocity of uniform flow ahead of shock-wave system
U_∞	free-stream velocity
W_1, W_2	point loads on beam
x	distance behind trailing edge
y	distance from center line of wake
γ_1, γ_2	ratio of specific heats in supersonic and subsonic stream, respectively (reference 14)
δ	semiangle of wedge or cone
ϵ	width of impulse-type wave (reference 14)
μ_1	coefficient of viscosity in uniform flow ahead of shock-wave system
ν	load ratio (W_2/W_1)
ρ_1	density in uniform flow ahead of shock-wave system

REMARKS ON SHOCK WAVES

In experimental measurements of the interaction between a shock wave and boundary layer it is important that the essential structure (i. e., pressure distribution) of the shock wave be known. This distribution may, for various reasons, not be the same as that expected from simple theory; the differences may be of the same order as the effects being measured in the interaction with a boundary layer. Some of the possible problems are discussed below and some measurements of shock structure are presented.

STEP WAVE[3]

In an ideal fluid the pressure field at a normal shock is a step distribution as indicated by the solid line in sketch (a). The pressure distribution through the inclined wave originating at a corner or at a wedge vertex (see sketch (b)) is also a step distribution. The thickness of the transition region is zero and the pressure gradient is infinite; the strength may be defined by the pressure ratio p_2/p_1.

[2] Some measurements on shock-wave reflection from a surface with turbulent boundary layer have been reported by Fage and Sargent (reference 11). The purpose of that investigation is, however, very different from the present approach.

[3] The term "step" wave will sometimes be used to distinguish it from the "impulse-type" wave referred to later.

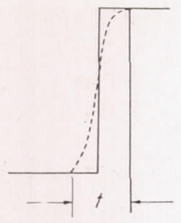

(a) Pressure profile through a step wave.

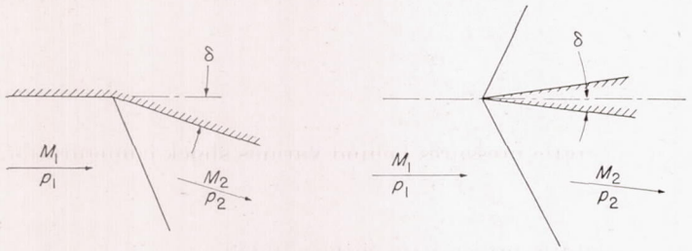

(b) Examples of step waves.

When account is taken of viscosity (and heat conduction), it is found that the distribution is similar to that shown by the dotted line (sketch (a)), so that a shock thickness t can be defined for the transition region; the pressure gradient then is of the order $(p_2-p_1)/t$. At a Mach number of 1.4, t is of order 10^{-4} centimeter and the pressure gradient is of order 10^4 atmospheres per centimeter while at a Mach number of 1.001, t is of order 10^{-2} centimeter and the pressure gradient is of order 0.1 atmosphere per centimeter; these values are for normal shocks. For inclined shocks, the thicknesses t are of the same orders, but (for corner or wedge angles of about 5°) the pressure gradients are one-tenth as large as those for normal shocks. (Density gradients are of the same orders as pressure gradients.)

Experimentally, stationary shocks can be observed only in the presence of boundaries, and boundaries introduce further viscous effects often greatly modifying the above theoretical results. For instance, consider again the examples of step waves (sketch (b)). If boundary-layer effects are neglected, then the shocks in both cases are identical for the same M and δ in each case. In a real fluid there is a boundary layer ahead of the corner shown at the left, the development of which has presumably started some distance upstream. The production of the shock wave at this corner involves a strong interaction with the boundary layer, and the two, shock wave and boundary layer, modify each other considerably. In the case shown at the right there is a viscous region near the wedge vertex which is quite different from the boundary layer in the corner. Again, there is a strong interaction between this viscous region and the shock which "originates" there, but the effects will, of course, be different from those at the corner.

Thus it can be expected that "clean" shock waves, having the theoretical pressure fields shown in sketch (a) of the pressure profile through a step wave, will probably be the exception rather than the rule.

In the case of the wedge, the effect of viscosity can be appreciated by the following example. Let the angle δ of the wedge decrease continuously to zero. Thus the wedge degenerates to a plane, along which the flow is still strongly retarded. In the neighborhood of the nose there must be a strong streamline curvature. This gives rise to some kind of pressure field (shock followed by expansion), extending from the nose in the general direction of the Mach lines. With no viscosity, there would not have been such a wave system. In this case, then, the effect of viscosity is very important. For further discussion of this, see reference 10.

The geometric conditions (e. g., small mechanical imperfections) may also be very important. Consider again a nonviscous flow, impinging on a wedge of semiangle δ (sketch (c)). The nose wave and a Mach wave from a point Q on the wedge intersect at a point P, defining a region OQP whose height is H_1. For small values of δ, $H_1 \approx b/\delta$ where $b=\overline{OQ}$.

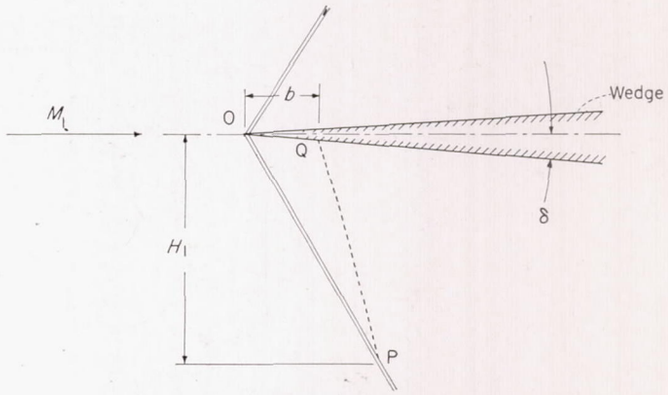

(c) Nonviscous flow impinging on wedge.

Now suppose OQ to be a small portion near the nose of a wedge. If there is a disturbance somewhere on OQ, then its zone of influence lies within the triangle OQP and so can also be characterized by the height H_1. Thus the effect of disturbances or imperfections near the nose will extend to distances inversely proportional to the wedge angle. In this case, the magnitude of the effect will depend principally on the amplitude of the disturbance. Such a disturbance might be caused by the viscous effect described above which, as has been seen qualitatively, also increases in importance with decreasing angle.

There is a third effect, that of nose bluntness (sketch (d)).

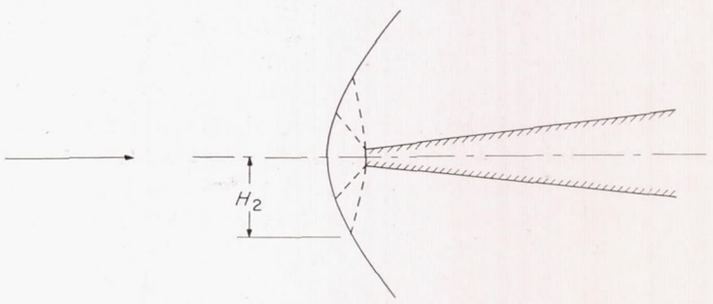

(d) Effect of nose bluntness.

This apparently cannot be treated in the same way as a disturbance on the side of the wedge. The schlieren pictures in figure 1 show the effect of bluntness of two wedges which differ only in nose radius. Evidently the extent of the

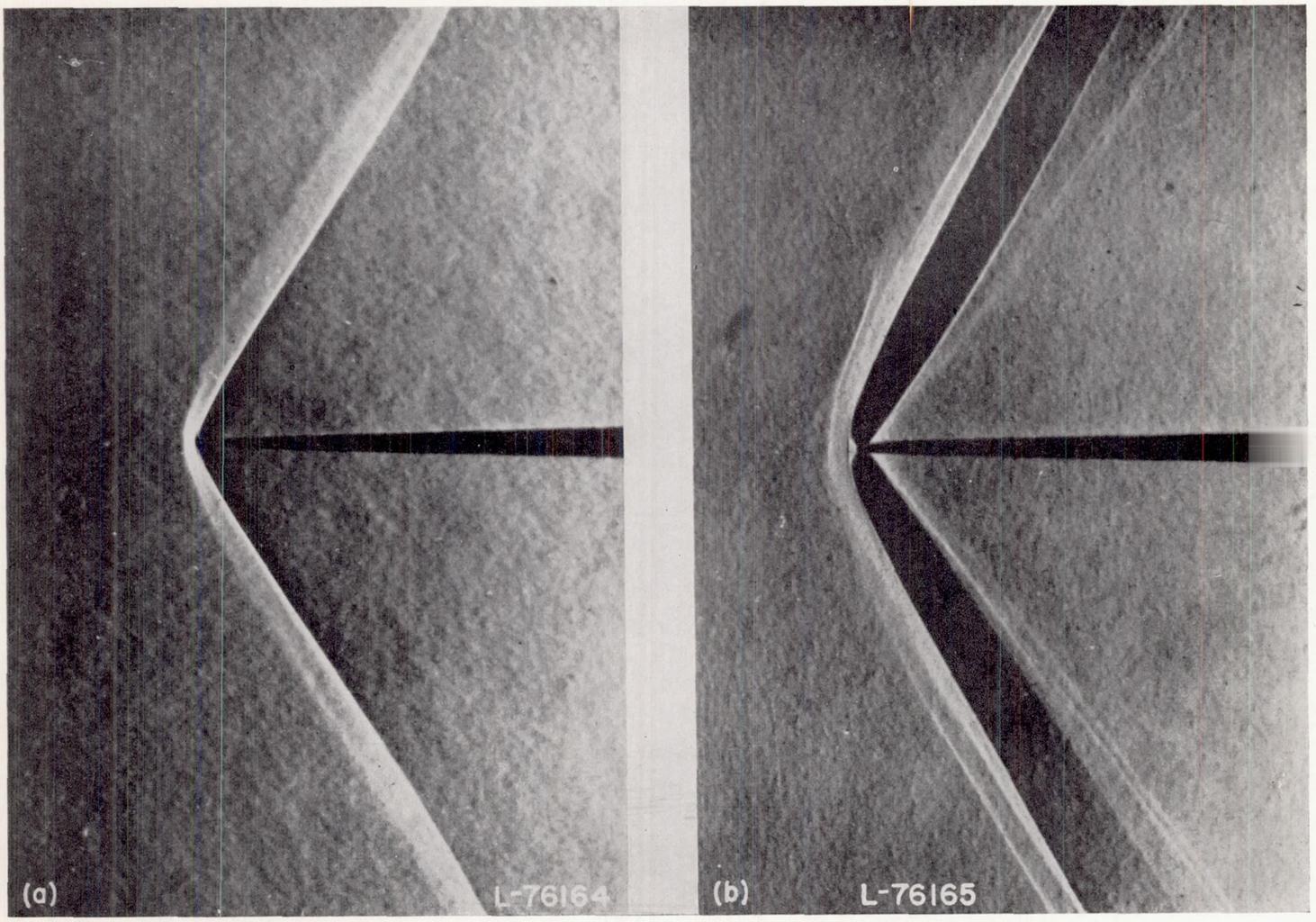

(a) Nose radius, 0 inch. (b) Nose radius, 0.005 inch.

FIGURE 1.—Effect of nose bluntness on shock wave from wedge (adapted from reference 6). $\delta=1.5°$; $M_1=1.2$.

region of influence depends on the nose bluntness as well as the angle of the wedge sides. The whole question of this effect is related to the problem of a detached shock in a viscous fluid; even qualitative estimates are very difficult. But, in general, this effect will also increase in relative importance if the wedge angle decreases and the Mach number approaches unity.

The effect of the wedge nose on the shock is visible in schlieren pictures. Almost invariably there is an expansion region following the shock near its origin at the nose. For instance, compare the pictures in figures 2(a) and 2(b) which show the effect of wedge angle. In the case for which $\delta=1.5°$ the nose effect can be seen to extend much farther than for the wedge of larger angle. (Both wedges have comparable nose bluntness.) On the other hand, the effect of boundary layer on a shock produced in a corner is evident in figure 3. Near the origin there is clearly a considerable difference in structure between shocks originating at a corner and those originating at a wedge.

Pressure measurements through shocks also reveal the effects described above. Figure 4 shows the pressure distributions through the shock from a 3° wedge, taken at two different heights. The apparent thickness of the shock shown by these measurements is not the thickness t referred to previously, which is several orders smaller, but rather is due to the turbulent boundary layer on the measuring probe. With a laminar boundary layer this apparent thickness is even much larger (cf. fig. 5).

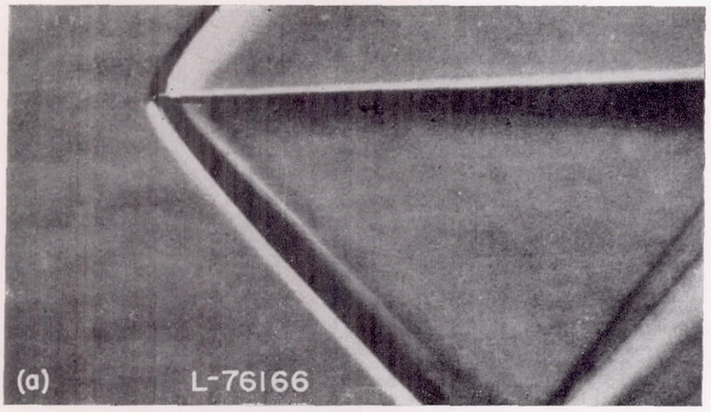

(a) Semiangle δ, 1.5°; nose radius, 0.005 centimeter; $M_1=1.44$.

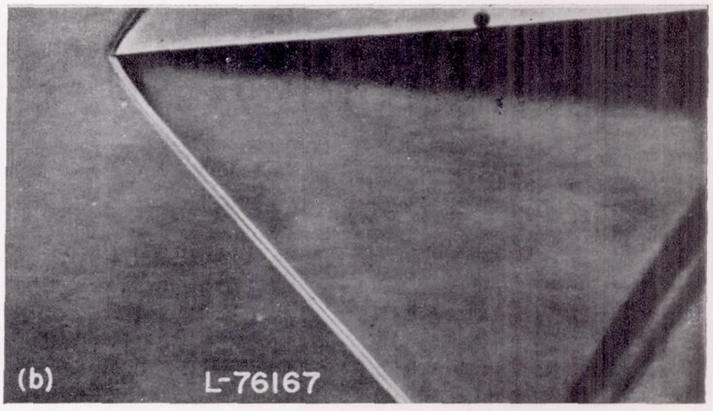

(b) Semiangle δ, 4.5°; nose radius, 0.005 centimeter; $M_1=1.44$.

FIGURE 2.—Effect of vertex angle on shock waves from wedges.

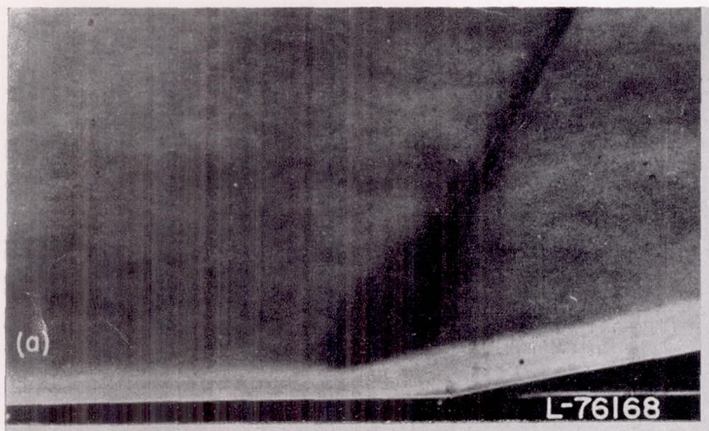

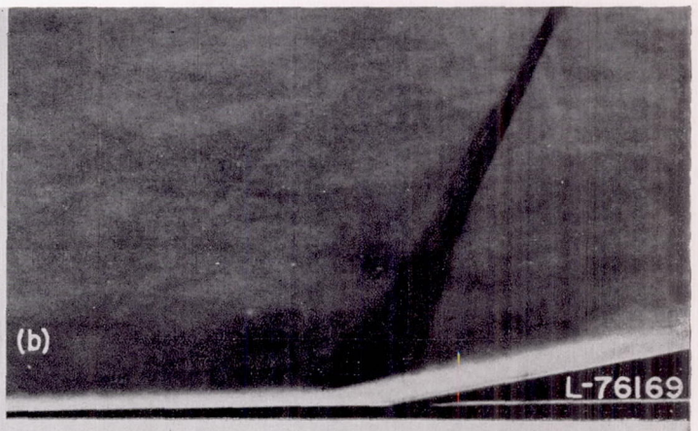

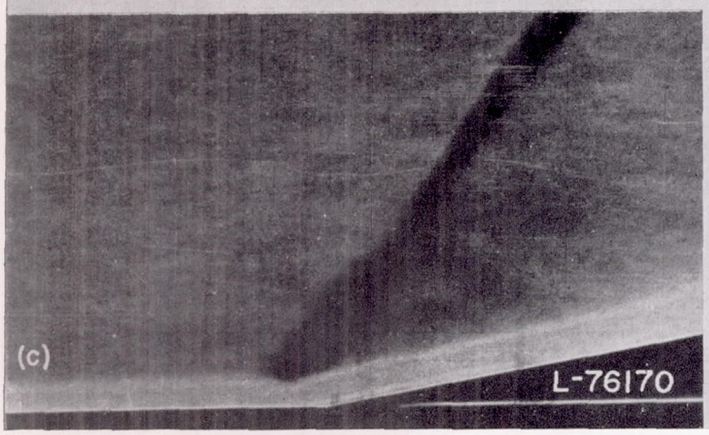

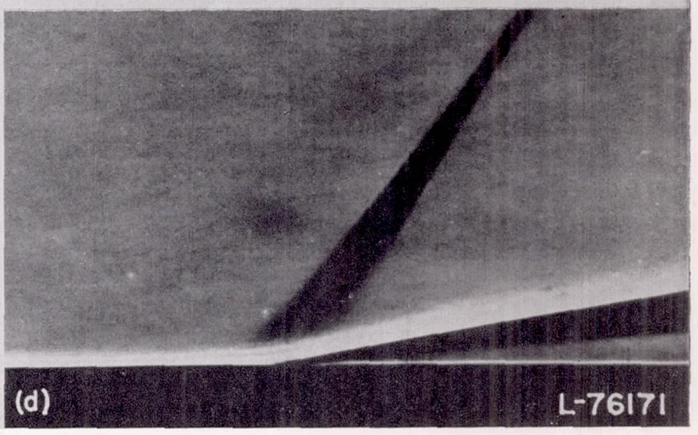

(a) Turbulent boundary layer; $M_1=1.42$.
(c) Turbulent boundary layer; $M_1=1.55$.

(b) Laminar boundary layer; $M_1=1.42$.
(d) Laminar boundary layer; $M_1=1.55$.

FIGURE 3.—Shock wave in a corner.

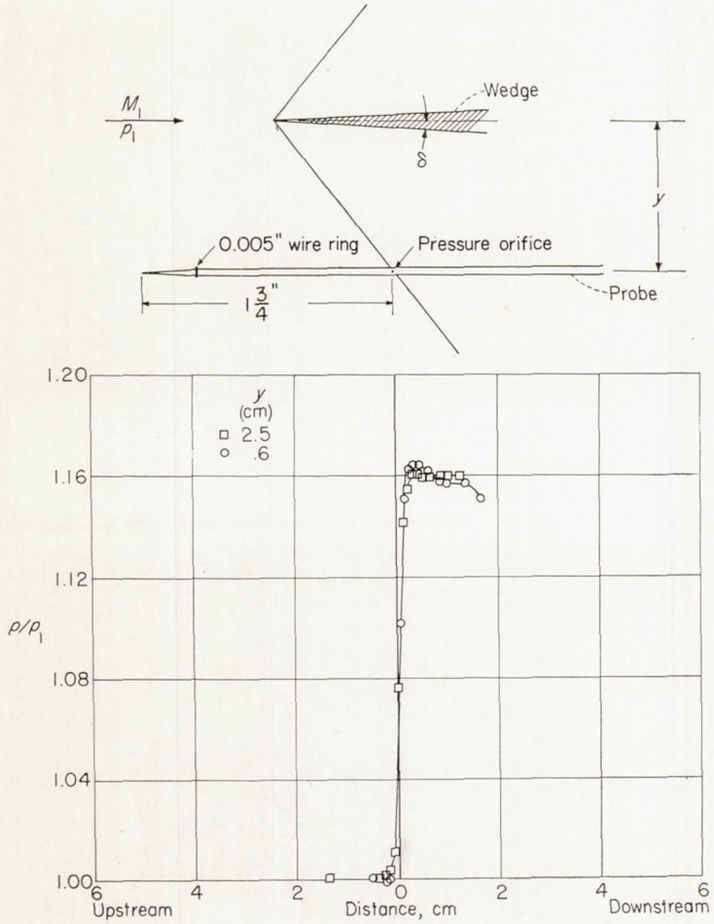

FIGURE 4.—Effect of distance from origin of shock wave. $\delta=3°$; $M_1=1.36$; probe boundary layer, turbulent.

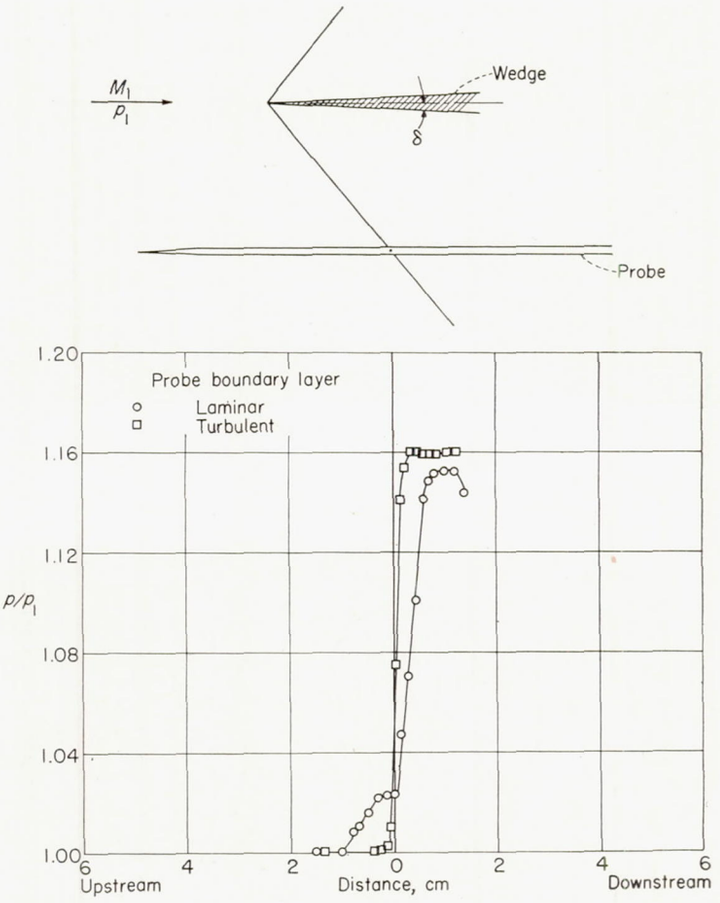

FIGURE 5.—Effect of probe boundary layer on static-pressure measurements through a shock wave. $\delta=3°$; $M_1=1.354$.

In all cases, the shock will be clean at distances sufficiently far from the point where they originate provided no other influences enter the field. The necessary distance at a given Mach number increases as the wedge (or corner) angle decreases and as wedge bluntness increases. Within the confines of wind tunnels and model configurations used in experimental work, it is sometimes not possible to produce shock waves sufficiently far from the region where they are to be used in an investigation; therefore, the above considerations are important.

CONICAL SHOCK WAVES

The pressure field of a cone in a nonviscous supersonic flow (sketch (e)) consists of a conical shock wave OA attached to the nose (for Mach numbers above the detachment Mach number) followed by an isentropic field of continuously rising pressure. "Rays" OM from the nose are isobars. A typical pressure distribution along a line AB in a meridian plane is sketched on the left. There is a jump in pressure p_w-p_1, through the conical shock, as in the case of the step shock from a wedge. But in the conical field the pressure continues rising after the initial jump until it reaches the value p_s at the cone surface. For small cone angles the initial pressure jump may be very small compared with the total pressure rise (e. g., for a 5° half angle cone at $M=1.4$,

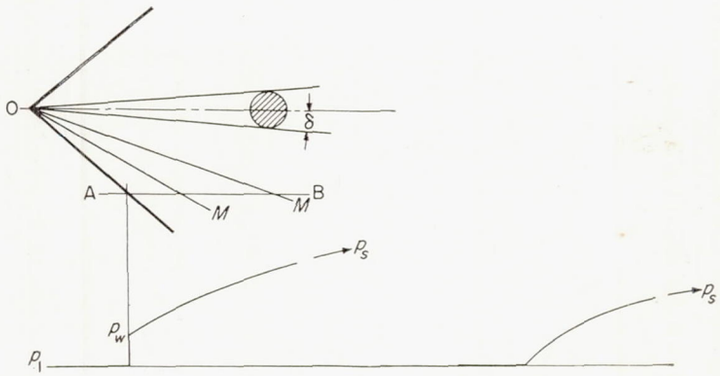

(e) Conical pressure fields.

$(p_w-p_1)/p_1$ is 4 percent of $(p_s-p_1)/p_1$[4] so that a distribution almost like that shown on the right is obtained.

The remarks made for the step wave apply also to the wave or pressure field due to a cone. The initial pressure jump, in particular, may be greatly modified by nose effects.

[4] Recent computations by Lighthill (reference 15) show that the deflection θ through the shock wave from a cone is proportional to the fourth power of the cone angle δ. This result, together with the well-known relation for the pressure coefficient for cones of small angle, leads to the following order-of-magnitude relations for cone shocks as compared with wedge shocks:

Relative total pressure change, $\left(\frac{p_s-p_1}{p_1}\right)_{\text{cone}} : \left(\frac{p_2-p_1}{p_1}\right)_{\text{wedge}} \approx \delta \log_e \frac{1}{\delta}$

Relative pressure jump through shock, $\left(\frac{p_w-p_1}{p_1}\right)_{\text{cone}} : \left(\frac{p_2-p_1}{p_1}\right)_{\text{wedge}} \approx \delta^3$.

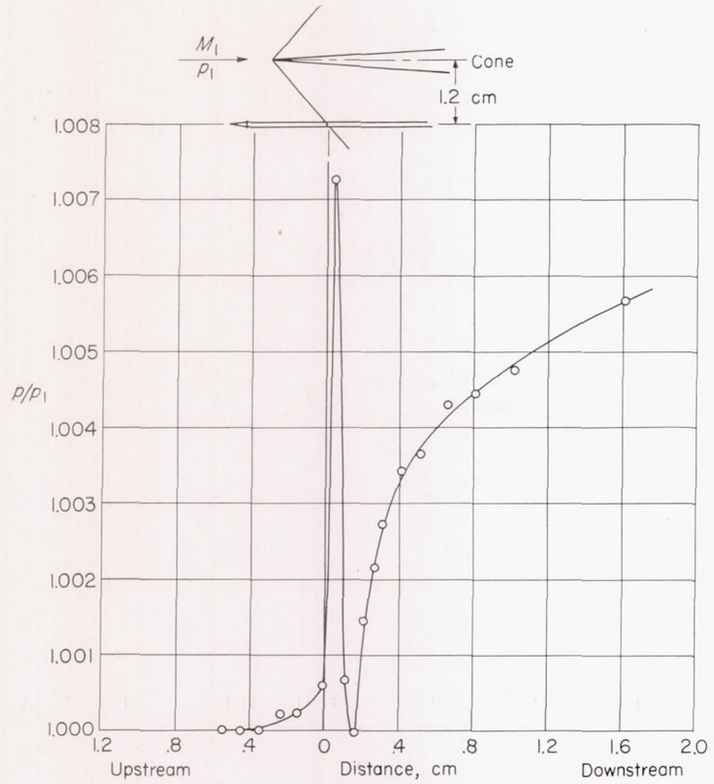

FIGURE 6.—Static-pressure survey through impulse-type wave from 2° cone. $M_1=1.32$; cone nose radius, 0.01 centimeter.

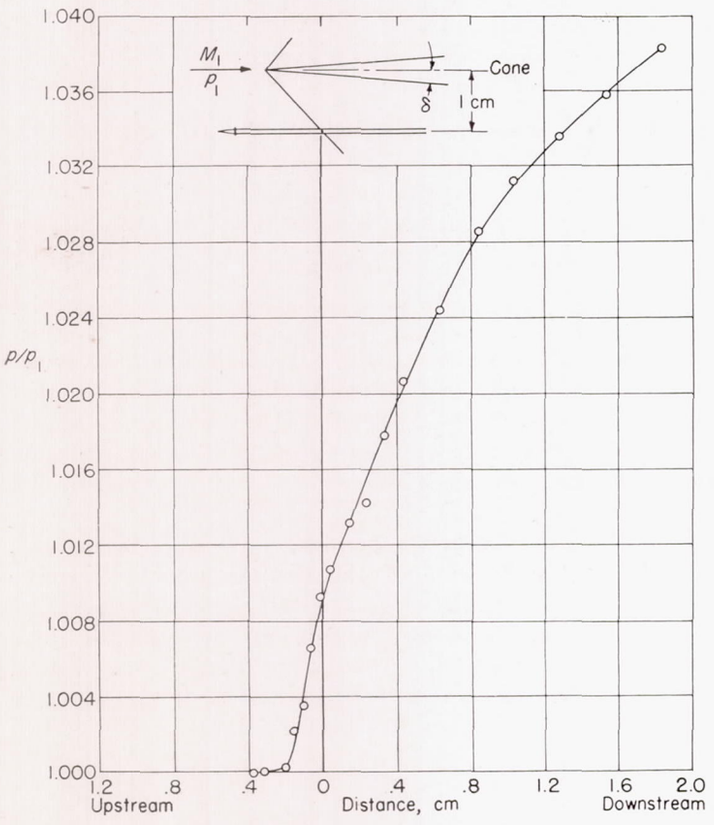

FIGURE 7.—Static-pressure survey through wave from 5° cone. $\delta=5°$; $M_1=1.32$; cone nose radius, 0.007 centimeter.

Figure 6 shows the measurement of a wave from a 2° cone and figure 7, that from a 5° cone, both of comparable bluntness. The greater nose effect on the 2° cone is clearly evident. The compression-expansion wave shown by the measurement can be seen in the schlieren picture of figure 8 (a). On the other hand, the wave is much cleaner from the 5° cone shown in figure 8 (b).

A point of interest is the following: To the pressure jump p_w-p_1 of sketch (e) there is a corresponding density jump $\rho_w-\rho_1$ that should be visible in a schlieren picture, which shows up density gradients. However, if this jump is very small, then the corresponding shock thickness t is relatively large and the density gradient is small, as shown above. Thus a clean cone wave will often not be visible at all in schlieren pictures (for cone angles less than about 5°). (See, e. g., fig. 8 (b).)

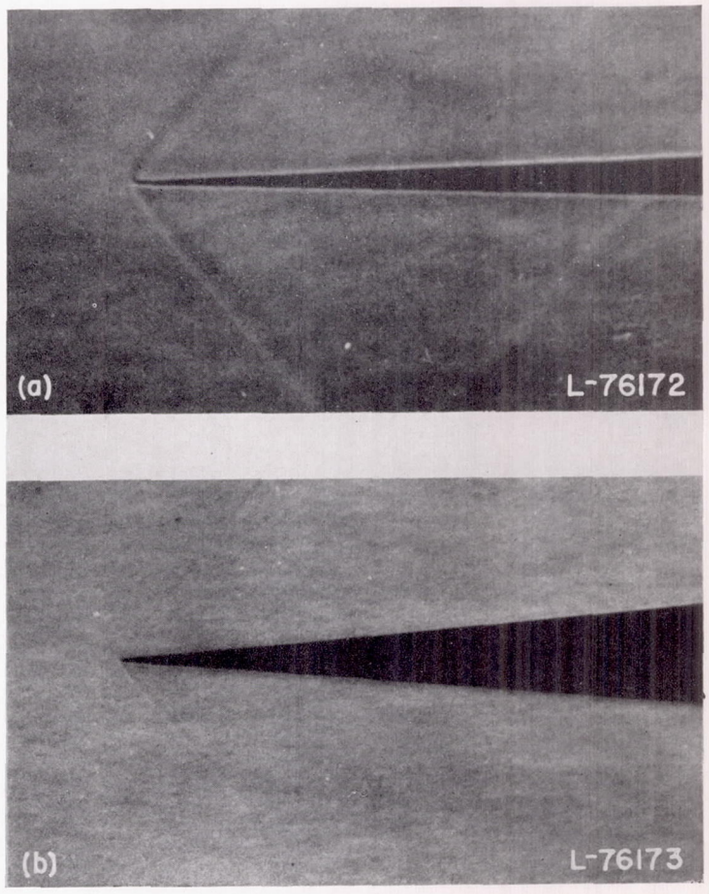

(a) Semiangle δ, 2°; nose radius, 0.01 centimeter; $M_1=1.32$.
(b) Semiangle δ, 5°; nose radius, 0.007 centimeter; $M_1=1.32$.

FIGURE 8.—Effect of vertex angle on shock waves from cones.

IMPULSE-TYPE WAVES

The term "impulse-type wave" will be applied to a pressure field consisting of a sharp compression immediately followed by an expansion (see sketch (f)). It may be two-dimensional or axially symmetric. The initial part of the conical wave shown in figure 6 is the impulse type. In this case, however, it is followed by a second compression. A two-dimensional impulse-type wave without a following

234476—53——2

compression can be obtained according to nonviscous theory by the method shown in sketch (f). After being deflected at the nose of a wedge, the flow is expanded around a corner until it is parallel to its original direction. Along the line AB, through the point of intersection of shock wave and expansion wave, the pressure distribution will be like that shown. For small wedge angles, $p_3 \approx p_1$.

A measurement of such an impulse wave is given in figure 9.

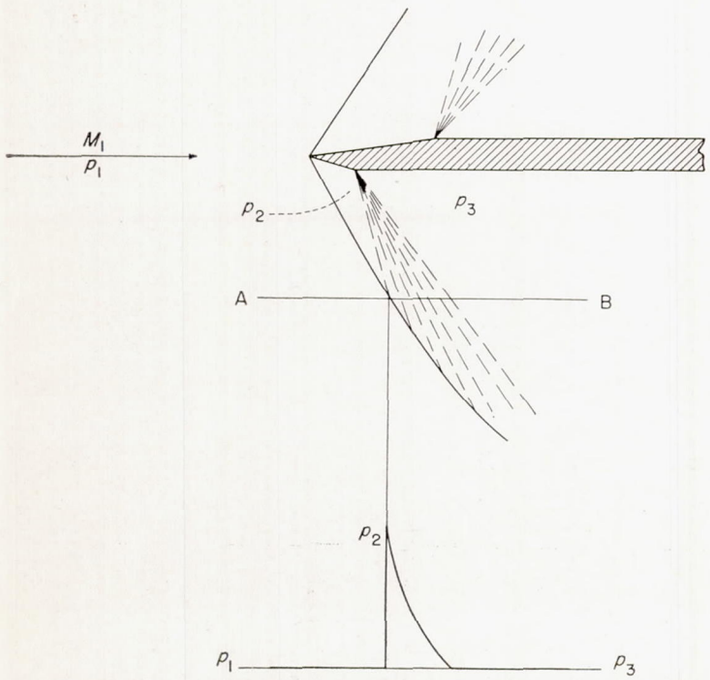

(f) Impulse-type wave.

GENERAL CONSIDERATIONS ON SHOCK-WAVE REFLECTION

REFLECTION OF INCLINED SHOCK WAVE FROM PLANE SURFACE

In nonviscous flow the simplest example of a shock reflection is that illustrated in sketch (g). The initial

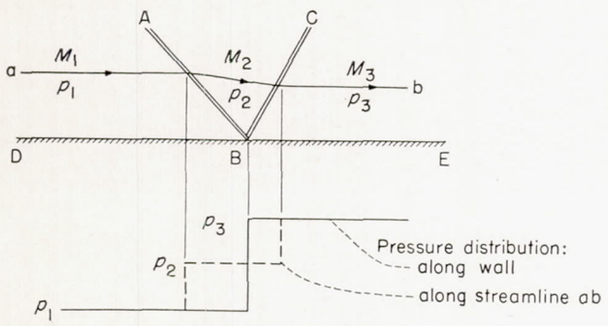

(g) Shock reflection in nonviscous flow.

two-dimensional flow, at Mach number M_1 and parallel to the wall DE, is disturbed by the incident straight compression

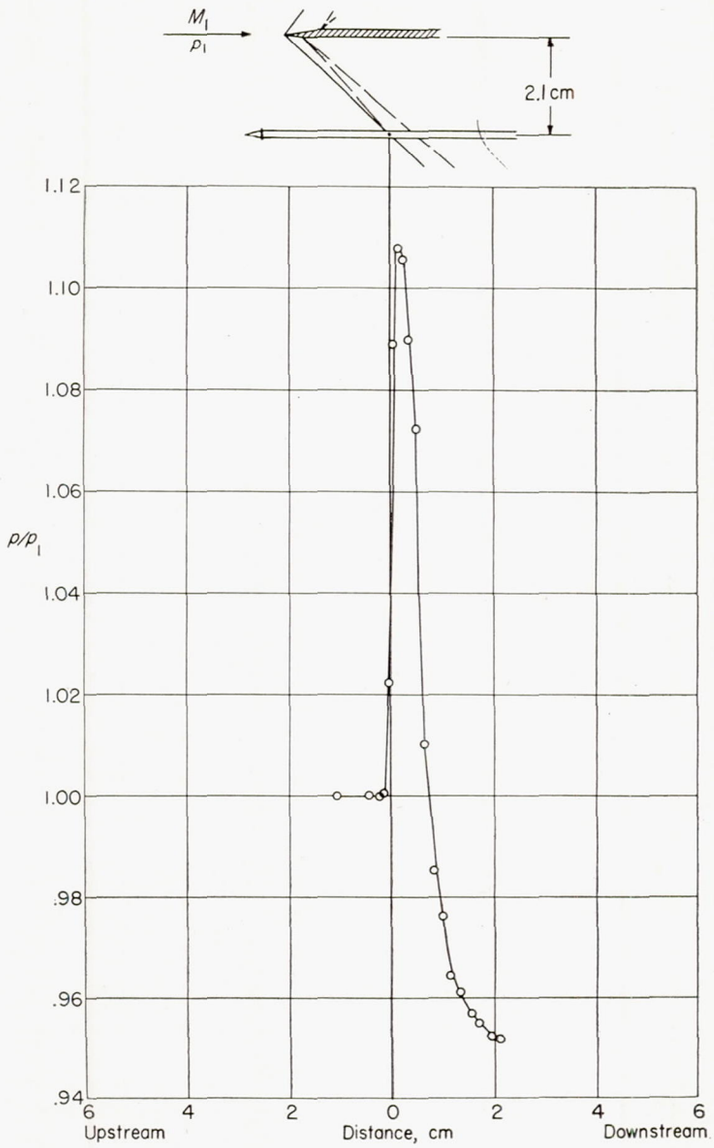

FIGURE 9.—Static-pressure survey through impulse-type wave. $M_1=1.38$.

step wave [5] AB of strength p_2/p_1. To make the flow downstream of B parallel to the wall, there must be another compression wave BC originating at B and having a strength p_3/p_2. The pressure distributions along a streamline ab and along the wall are shown in the sketch by dashed and heavy lines, respectively.

The strength p_2/p_1 of the incident wave may be defined, instead, by the angle δ of the disturbance supposed to produce it (see, e. g., sketch (b)). For a given δ the pressure ratios across the shock p_2/p_1 and across the reflected wave p_3/p_1 will vary with M_1. Curves for the pressure ratios, which are easily calculated from a shock polar, are given in figures 10 and 11. Figure 10 shows the limit for an attached

[5] See section "Remarks on Shock Waves."

shock. Correspondingly, there is a limit for a simple, or regular, reflection (fig. 11). For values of M_1 below this limit the reflection is the so-called "Mach reflection" (see section "Mach reflections").

In a real flow, there is a boundary layer (laminar or turbulent) on the wall. This modifies the simple reflection pattern and the pressure distributions shown in sketch (g).

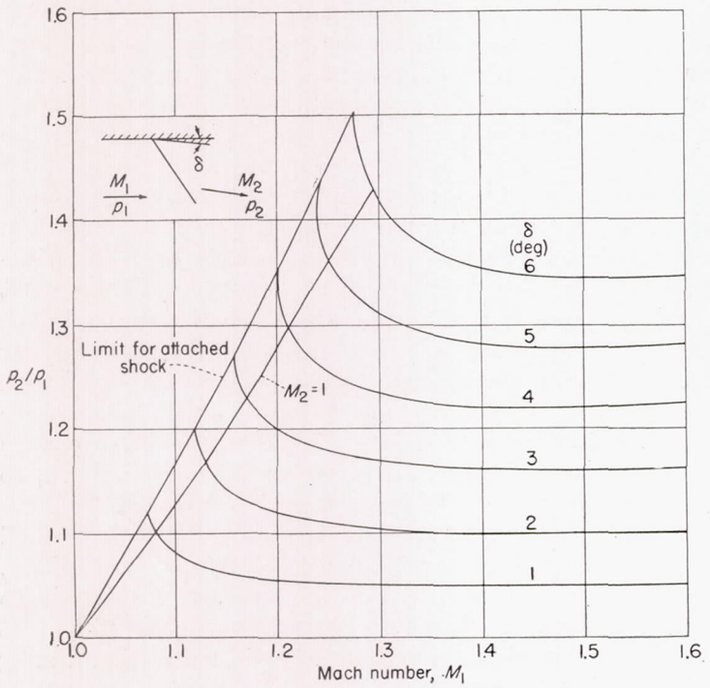

FIGURE 10.—Pressure ratio across inclined shock.

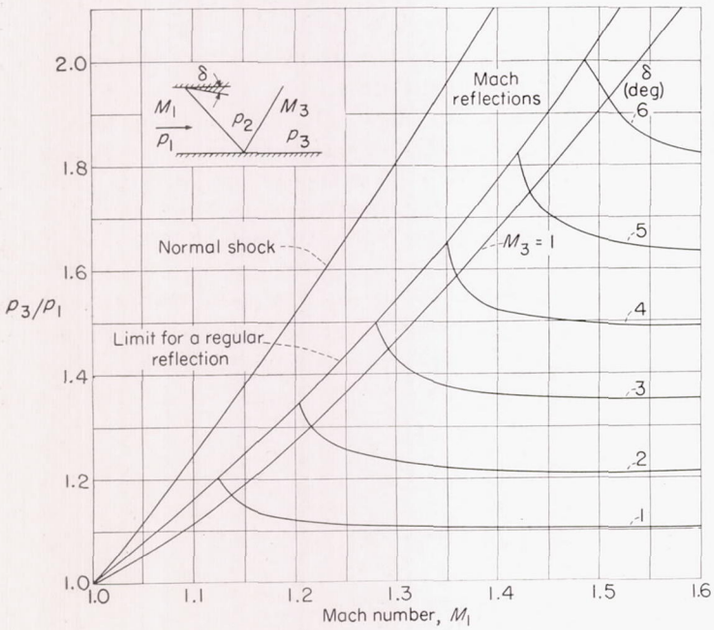

FIGURE 11.—Pressure ratio across regular reflection.

The experiments reported below are concerned principally with detailed measurements of these reflection patterns and pressures in the presence of turbulent and laminar boundary layers.

One of the most striking features is the difference in effects obtained with turbulent and laminar boundary layers, respectively (fig. 12). This difference was first observed in

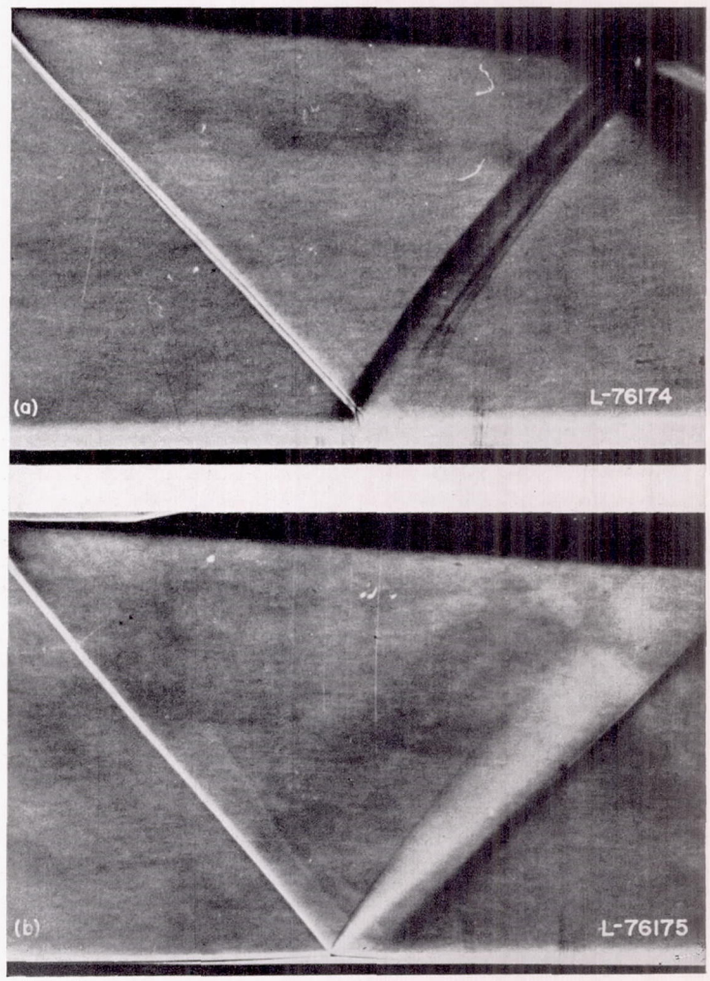

(a) Turbulent boundary layer.
(b) Laminar boundary layer.

FIGURE 12.—Typical shock-wave reflections from flat surface with boundary layer.

experiments on transonic regions (references 3 and 5). However, in the transonic case, the "incoming" shock, at some distance from the boundary layer, actually depends on the boundary layer, as well as on the flow field, and cannot be controlled independently. Therefore it is difficult to study the effect of the boundary layer itself.

In some early investigations into the configuration corresponding to that shown in sketch (g), an inclined shock wave was produced by a wedge and allowed to intersect a flat surface. Pictures of the reflection patterns for turbulent and laminar boundary layers were presented in reference 6, together with a qualitative discussion of the phenomena.

Some more recent schlieren photographs of the typical patterns are reproduced in figures 12 (a) and 12 (b). Roughly, the appearance of the reflections is always as follows:

With a turbulent boundary layer (fig. 12 (a) and sketch (h)), there is a thickening of the layer immediately upstream of the point of intersection with the shock. The compression field due to this thickening modifies the shape of the incident and reflected waves in the neighborhood of the point of intersection.

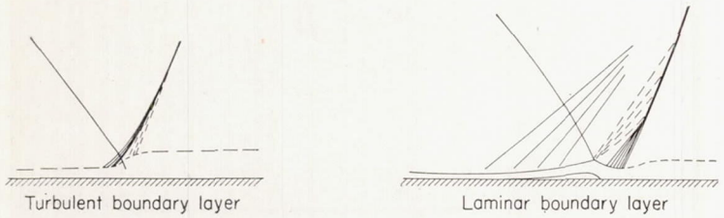

(h) Reflection patterns.

With a laminar boundary layer (fig. 12 (b) and sketch (h)), the thickening is not so abrupt but begins upstream at a distance which may be of the order of 50 boundary-layer thicknesses (as compared with about 5 in the turbulent case). The compression field due to this thickening is greater in extent and not so concentrated as in the turbulent case. Near the point of intersection, the incident wave reflects as from a free jet surface and the boundary layer has a "corner," which is also the vertex of an expansion "fan." After the corner there is a strong curvature in the boundary layer giving rise to a second compression region. Transition may or may not occur following the reflection process, depending on the Reynolds number, strength of incident shock, and so forth.

Far from the surface, the incident and reflected waves should be like those predicted by the simple nonviscous theory; the compression and expansion regions must combine to give "in the large" the same simple pattern (see, e. g., sketch (b)) for both turbulent and laminar boundary layers.[6] But in the interaction region (which may extend to several hundred boundary-layer thicknesses) it seems evident that the differences are more than differences in scale and that the descriptions of the two phenomena may differ essentially.

Before presenting the measurements obtained for reflections corresponding to the regular case (see sketch (g)), a better perspective will be obtained by considering briefly some of the other cases of shock reflection that may occur.

OTHER SHOCK-REFLECTION CONFIGURATIONS

Normal shock near a wall.—Since, by definition, a normal shock is perpendicular to the direction of flow, the flow conditions through a normal shock near a wall are satisfied without the introduction of any other shock or discontinuity; that is, there is no reflection. (See sketch (i).) The theoretical surface pressure distribution is then a pressure jump

[6] In most practical cases, however, the distances cannot be freely chosen but are governed by other characteristic length parameters entering the problem, for example, wind-tunnel size, height of a supersonic zone, and so forth. For such cases the reflection process in the real fluid may differ essentially from the ideal-fluid case.

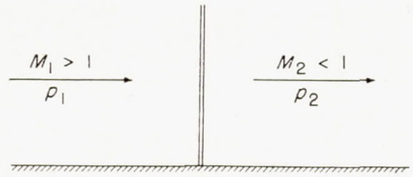

(i) Normal shock near a wall.

like that across the reflection of an inclined shock. For flow past a straight wall the pressure jump at a given Mach number is higher through a normal shock than through any other reflection pattern.

An important property of the normal shock is that the Mach number M_2 of the flow after the shock is less than unity; the normal shock separates a supersonic field from a subsonic one. Since the field downstream is subsonic, it is not possible to describe a normal-shock configuration without specifying the "conditions at infinity," whereas most regular reflections can be discussed by considering only the completely supersonic field near the point of reflection. For this reason experiments on interaction of a normal shock with boundary layers may be somewhat more difficult than those with a regular reflection, for the interaction may change conditions at infinity, thus changing the normal shock, so that the latter cannot be independently controlled.

Actually, even for "regular" reflections there is a small range of Mach numbers M_1 for which $M_3<1$ (see fig. 11), that is, for which the field after the reflection is subsonic, so that such configurations must be affected by conditions at infinity. This will be discussed below in the section dealing with Mach reflections.

Examples of normal, or near-normal, shocks at a wall may be observed experimentally in transonic regions (figs. 11b and 11c in reference 5), ahead of a choked duct (fig. 13 (a)), and at the base of a Mach reflection (see sketch (j)). Normal-shock segments also occur in many other flow patterns, for example, in detached shocks.

Mach reflections.—In figure 11, between the line for a normal shock and the line showing the limit for a regular reflection, is the region of Mach reflection. In a Mach reflection (sketch (j)) the incident wave branches, at some point P above the surface, into a "reflected" wave PC and a nearly normal wave PB (usually curved). The entropy changes across APC and across PB are different, but the pressure ratios and the flow directions must be the same. Therefore there must exist a velocity discontinuity, or vortex sheet, PS extending downstream from P. These features of

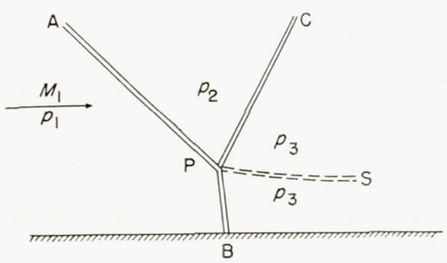

(j) Mach reflection.

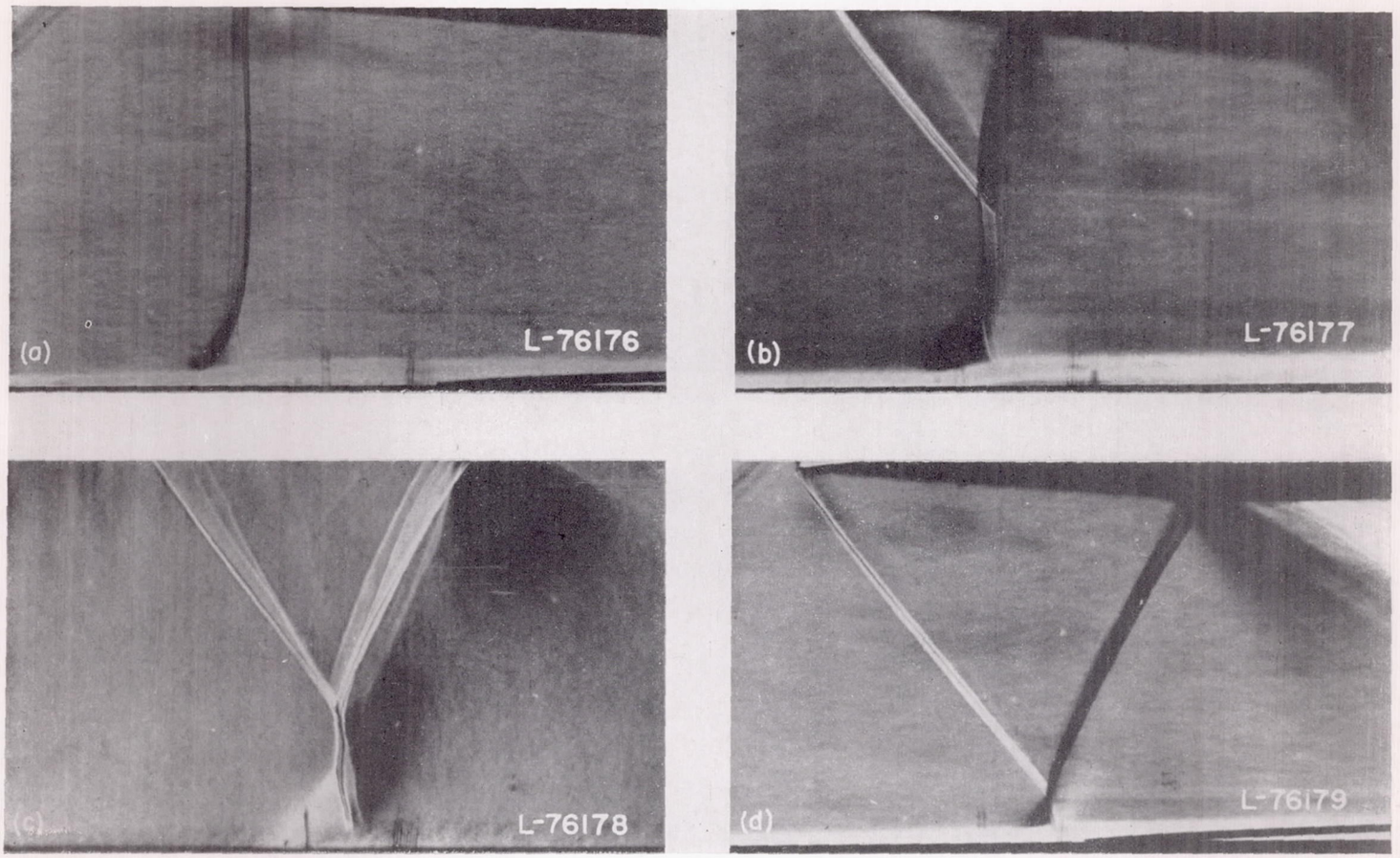

(a) Normal shock at mouth of duct.
(b) Mach reflection.
(c) Mach reflection.
(d) Regular reflection.

FIGURE 13.—Bifurcation at base of shock-wave reflection.

a Mach reflection are evident in the schlieren picture of figure 13 (b).

At least a portion of the flow downstream of a Mach reflection is subsonic, and therefore the configuration is not independent of conditions at infinity. The same is true also of regular reflections in the region to the left of $M_3=1$ in figure 11.

Since Mach reflections and normal shocks occur, as well as regular reflections, and since their regions of definition are not clear-cut, especially in the presence of boundary layers, it is useful, in an experimental investigation, to keep in mind their characteristics.

Bifurcated shocks.—A phenomenon frequently observed near the intersection of a shock with a wall is an apparent branching of the shock, or "bifurcation," near its base (sketch (k) and fig. 13). An investigation into this phenomenon was made by Fage and Sargent (reference 11) with some measurements on the interaction of shocks with a turbulent boundary layer in a nozzle.

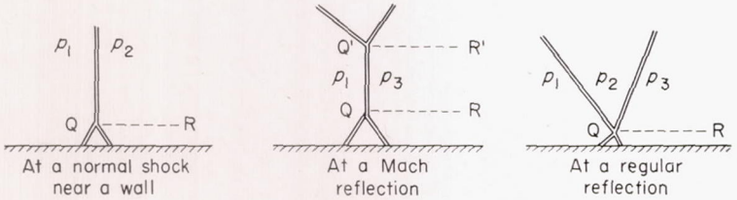

(k) Bifurcated shocks.

The configuration sometimes looks much like the triple-shock configuration of a Mach reflection (but inverted) and there is usually a vortex sheet QR extending downstream from the branch point. However, the reasons for the existence of the two cases are different. The Mach reflection is the triple-shock configuration that must exist when a regular reflection is not possible, and it does not depend on the presence of a boundary layer on the wall. On the other hand, the bifurcation depends entirely on the boundary layer. The pressure rise across the shock system separates (or thickens) the boundary layer ahead. This deflection of the boundary layer gives rise to an oblique compression shock (or continuous compression) which is the front leg of the bifurcation. The other leg must exist to give proper continuity of flow direction and pressure, as explained above. (Also note next paragraph.) Thus, bifurcation may occur at the base of a normal shock, a Mach reflection, or a regular reflection (fig. 13).

It does not seem too instructive to study the bifurcation from the point of view of the geometric conditions which must be satisfied. The "branches" of the bifurcation are more likely to be continuous compression regions than sharp shocks and so do not give the triple-shock configuration in the sense that a Mach reflection does.

Reflection of conical shock waves.—The conical pressure field due to a cone in a nonviscous supersonic flow has been discussed in the section "Remarks on Shock Waves" and is there illustrated by sketch (e). If a flat surface is placed along AB, then, to turn the flow parallel to AB, there must be a continuous reflection pattern behind the hyperbola of intersection through A. The theoretical analysis of this reflection is difficult (e. g., reference 16, p. 416) and has apparently not yet been completely worked out. However, it seems reasonable that, qualitatively, the surface pressure distribution, along a meridian, will also look like that of sketch (e) but with ordinates approximately doubled. In the experiments described below, cones were found useful to produce pressure fields like that on the right of the sketch, having no steep front. In this way the effect of pressure gradient on the boundary layer can be studied.

Reflections of shocks from curved surfaces.—The reflection of a curved shock or pressure field from a plane surface is, in a way, an inverse problem to that of reflection of a plane shock from a cylindrical surface. Here, again, there are apparently no cases theoretically worked out. In pressure-probe measurements through shock waves, theoretical results would be useful in evaluating the error due to the reflection of part of the shock from the probe surface (without, at first, taking account of the interaction with the boundary layer on the probe). The problem is that of the reflection of a plane shock from a circular cylinder.

Reflection of an impulse-type wave.—If a weak impulse-type wave, having the form shown in sketch (*l*), is reflected

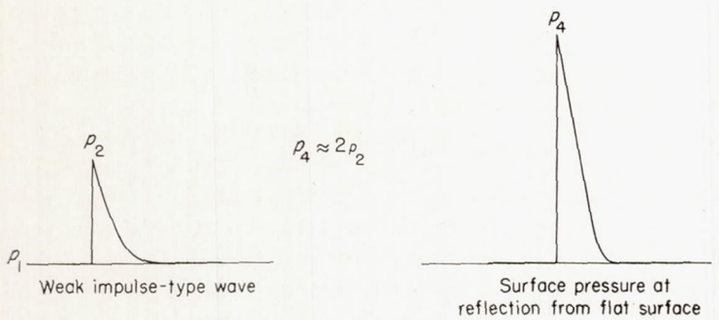

(*l*) Reflection of weak impulse-type wave.

from a flat surface, then the surface pressure distribution near the "point" of reflection will look like that on the right of the diagram (cf. reference 14).

The reflection of a strong impulse-type wave cannot be treated by a linearized theory. However, it can be expected that qualitatively it will be, in general, similar. On the other hand, viscosity (i. e., boundary layers) will probably modify the distribution in an important manner. The effect of the boundary layer on an impulse-type wave is studied in the experiments reported below.

EXPERIMENTAL SETUP

WIND TUNNEL

The measurements were made in the GALCIT 4- by 10-inch tunnel. (See fig. 14.) This tunnel is a continuously operating tunnel with Mach numbers in the supersonic range from $M=1.1$ to $M=1.55$. The tunnel incorporates a flexible nozzle of very simple design and a traversing system which traverses continuously in two directions. The tunnel, the flexible nozzle, and its performance are briefly described in the appendix.

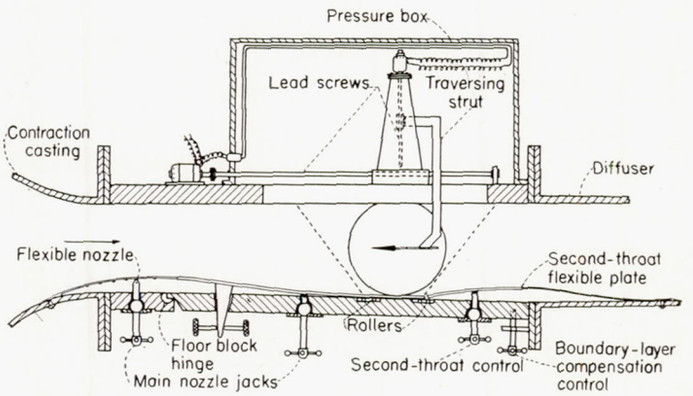

FIGURE 14.—Sketch of GALCIT 4- by 10- by 48-inch transonic-tunnel test section.

SCHLIEREN SYSTEM

Schlieren photographs were taken using spark exposures of a few microseconds' duration. The phenomena observed are, however, very steady and the photographs correspond to the respective pressure distributions. Spark exposures are advantageous in eliminating any lack of resolution due to oscillation of the schlieren system during exposure. An idea of the limit of resolution may be obtained from figure 8 (b), which shows a conical shock having a density gradient of about 0.01 atmosphere per centimeter.

PRESSURE PROBES

Static pressure within the field of flow was measured using a static tube of 0.05-inch outside diameter with a pointed tip and two 0.014-inch-diameter orifices approximately 2 inches from the tip. It was found important for accurate measurement of steep pressure gradients to make the boundary layer on the tube turbulent. This was accomplished by a ring of 0.005-inch wire around the tube about 0.2 inch rearward of the tip of the probe. The importance of this precaution can be seen from a sample measurement as presented in figure 5. Stagnation pressure

was measured with a probe made from a hypodermic needle flattened at the mouth. The pertinent dimensions are given in figure 15.

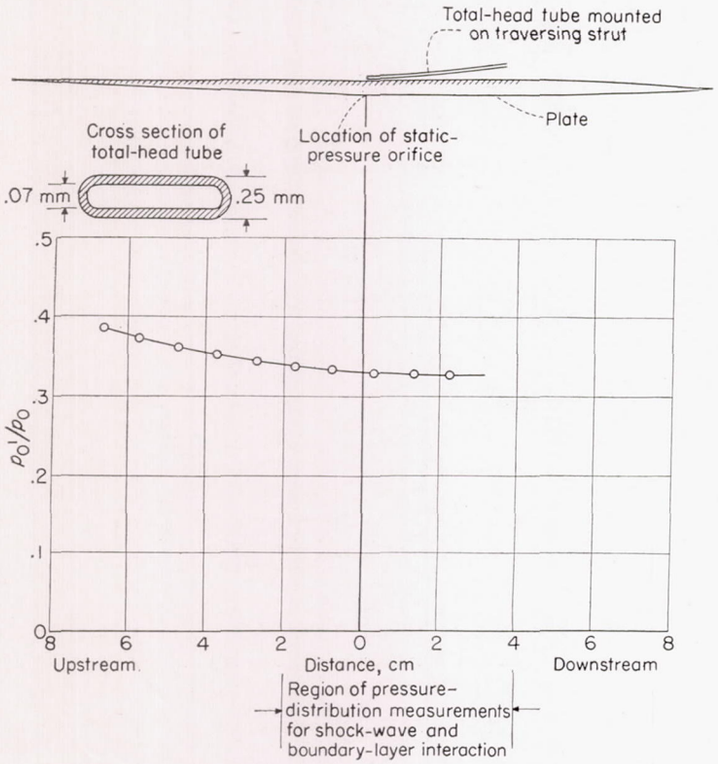

FIGURE 15.—Variation of total head along flat surface with laminar boundary layer. p_o', pressure indicated by total-head tube; p_o, stagnation pressure.

SHEAR LAYERS

A great deal of effort was spent in trying to produce supersonic shear layers. It was first attempted to obtain a shear layer in the wake of a curved shock wave. Here the entropy change, variable from point to point on the wave, produces a wide slipstream, that is, a shear layer. This method is clean and elegant but at the Mach numbers which could be reached ($M<1.6$) the possible variations of entropy and, therefore, of velocity in the shear layer are too small to be used for an investigation of reflection processes.

Wire grids of uneven spacing were next tried. Here the difficulty arose that the velocity distribution behind such a grid was not smooth and varied rapidly in the downstream direction. Furthermore, the losses in the production of the shear layer were so great as to bring the tunnel near the choking condition and hence manipulation with a wedge and shock waves was not possible.

The wake from a flat plate was found to be the best way under the present conditions to produce a shear layer. The wake has the disadvantage that the velocity distribution is not monotonic and the reflection characteristics are therefore more involved.

REFLECTION OF SHOCK WAVES FROM BOUNDARY LAYERS (MEASUREMENT OF SURFACE PRESSURES)

A shock wave from a wedge or cone is allowed to intersect the flat surface of a plate. (See sketch (m).) The plate is

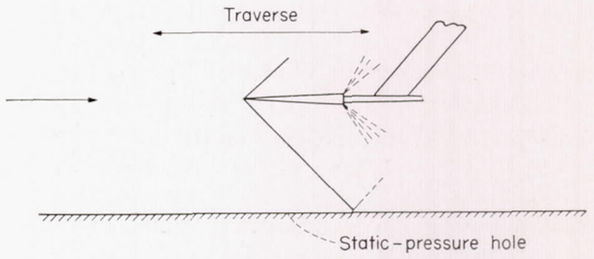

(m) Intersection of shock wave from wedge or cone with plate.

supported from the side walls, and its angle of attack relative to the flow direction is adjustable. The wedge or cone is mounted on the strut attached to the traversing carriage (fig. 14) so that its position, vertical or horizontal, can be varied continuously during operation. With this arrangement the incident shock wave can be moved back and forth over one of the static holes in the surface of the plate. Thus the pressure ahead of and behind the point of intersection is measured at a single static hole as the shock wave passes over it. This is equivalent to fixing the shock and taking measurements on a series of static holes in the vicinity of the intersection, provided the boundary-layer characteristics are constant, or nearly constant, over the region traversed. At the position where most of the measurements were made ($R=0.9\times10^6$) there is little change in the boundary layer over the measuring region (e. g., fig. 15). The error increases for measurements nearer the leading edge of the plate, but then another effect (see "Remarks on Boundary Layers in Supersonic Flow") becomes even more important.

This method has several advantages: In the first place, attaching a wedge or cone to the traversing strut is considerably easier and faster than supporting it from the walls (in the present test section). Secondly, there is no need to correct for reading differences in a series of static holes and there is no scatter in the readings. Some of the small pressure gradients measured would be completely obliterated by the differences that can be expected between different holes. Furthermore, it would be impossible to place, within the small regions investigated, a sufficient number of holes. Finally, it is quite convenient, experimentally, to make all

readings on a single manometer without switching devices and so forth. Some error could be introduced by reflection of tunnel waves from the wedge, as the latter moves forward. Comparing results of various runs made, for example, with the wedge at two different heights, indicates that this effect was not important in the measurements presented here.

Changes in the vertical and horizontal positions of the wedge or cone can be made to within 0.01 centimeter. Pressures are measured on mercury and on alcohol manometers, depending on the magnitudes of the pressure changes being studied. The accuracies are about 0.01 centimeter of mercury and 0.1 centimeter of alcohol, respectively.

In studying the effects of turbulent and laminar boundary layers, the turbulent boundary layer was obtained by stretching a very thin wire across the surface of the plate near its leading edge. A more detailed discussion of the boundary layer is given in the section "Remarks on Boundary Layers in Supersonic Flow."

MEASUREMENTS OF TOTAL HEAD

The same technique as described in the preceding section was used to measure total head very near the surface. A total-head tube with a flat narrow mouth (figs. 15 and 16) was fixed to the surface of the plate. Distribution of total head near the surface was then measured by moving the interaction zone back and forth over it, as described above.

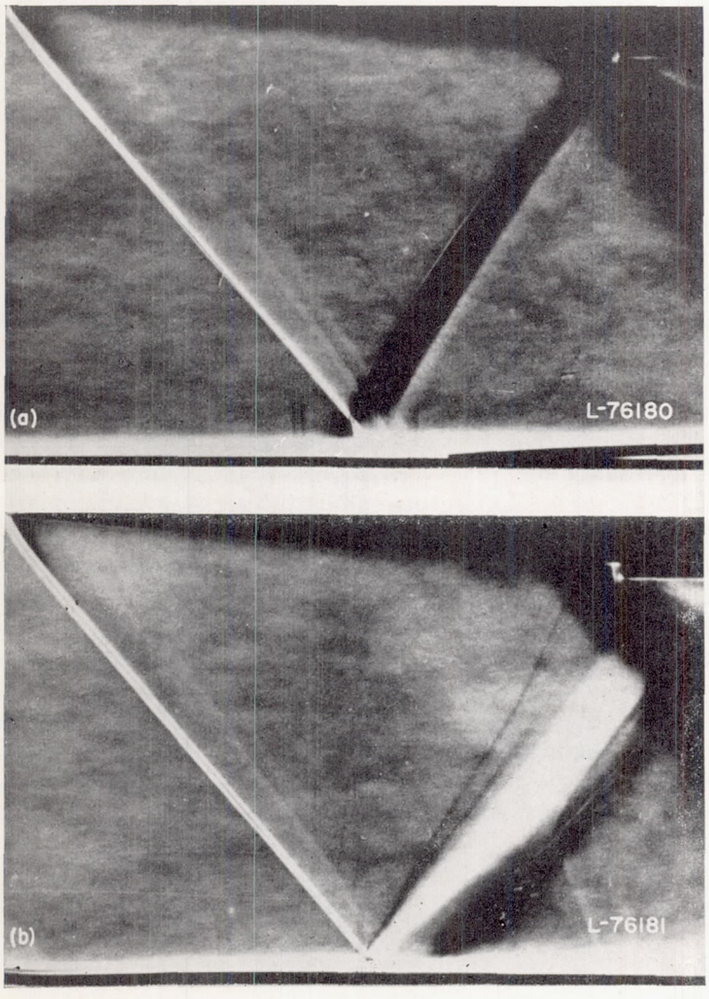

(a) Turbulent boundary layer. (Total-head tube visible in boundary layer, at lower right corner of picture.)
(b) Laminar boundary layer.

FIGURE 16.—Reflection patterns of 4.5° shock wave. $M_1=1.44$.

BOUNDARY-LAYER PROFILES

Measurements of total head at various heights in the boundary layer were made with a total-head tube which was set at various heights by means of the traversing strut. There was no vibration of the tube. Typical profiles, computed from these measurements, and dimensions of the probe are shown in figure 17.

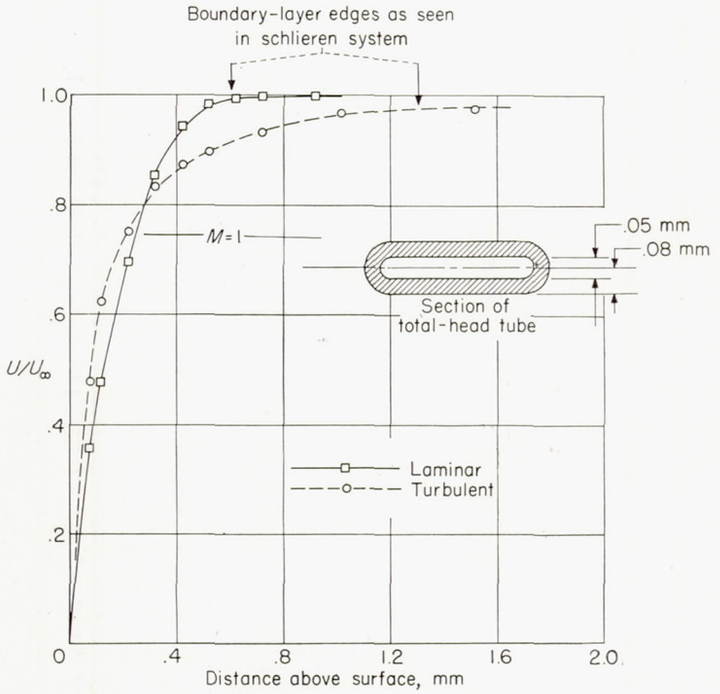

FIGURE 17.—Boundary-layer profiles on flat surface. $M=1.46$; $R=0.9\times10^6$.

PRODUCTION OF SHOCK WAVES AT A CORNER

Pressure distributions in the vicinity of a corner in supersonic flow were obtained by a similar method. A wedge, forming a corner at its line of contact with the plate (fig. 3), is moved back and forth, by the traversing strut, relative to a fixed static hole on the plate. This gives the pressure distribution ahead of the corner.

VISUALIZATION OF TRANSITION IN BOUNDARY LAYERS

Essentially, the technique used for visualization of transition in boundary layers is similar to the contamination and evaporation techniques used by British investigators. (See reference 17 for a summary.) The polished flat plate used for the boundary-layer and surface-pressure measurements was coated with a very thin film of machine oil. During operation, this film of oil would catch the very fine particles of dust present in the air. Probably because of the very much greater diffusion or turbulent mixing which occurs in the turbulent boundary layer, the regions of the plate with turbulent flow are coated with the dust particles and appear dull as compared with the shiny appearance of the portion with laminar boundary layer. Figure 18 shows the traces of typical patterns. It was found that the demarcation of

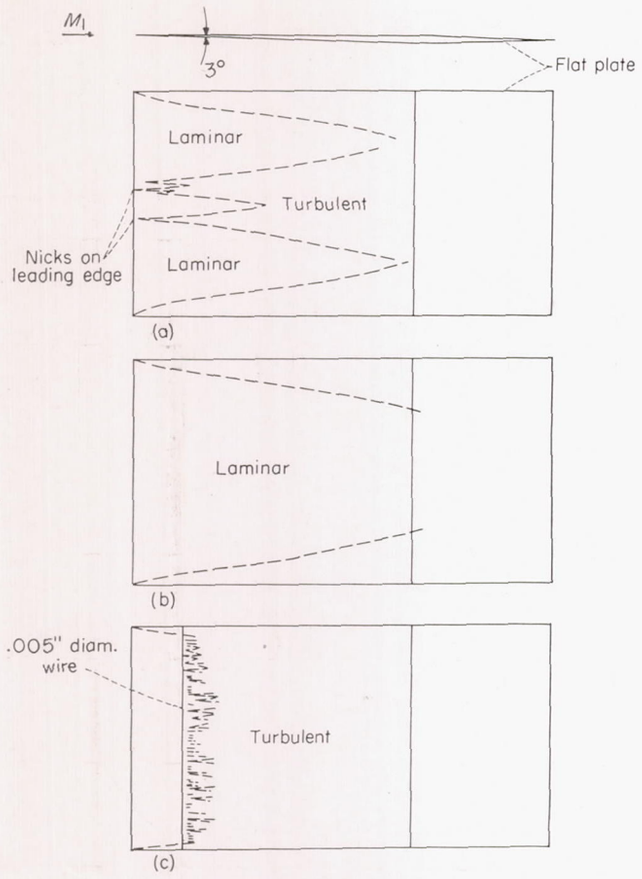

(a) Effect of leading-edge imperfections.
(b) Laminar pattern showing contamination from sides.
(c) Turbulent pattern (with wire).

FIGURE 18.—Stain patterns showing transition on flat surface. $M_1 \approx 1.40$; $R \approx 10^5$ per centimeter; width of plate, 10 centimeters.

the two regions became more pronounced if the tunnel was operated momentarily with condensation. That the two regions observed really distinguished the laminar and turbulent types of boundary-layer flow was confirmed by:

(1) Profile measurements in the two regions (fig. 17).

(2) The fact that the observed laminar type could be changed into the turbulent type either by raising the Reynolds number of the flow or by introducing disturbances on the surface of the plate.

RESULTS OF MEASUREMENTS OF SHOCK-WAVE AND BOUNDARY-LAYER INTERACTION

In this section, surface pressure distributions are presented for several cases of shock-wave and boundary-layer interaction, together with related measurements. The results for the cases investigated are quantitative. However, there is no attempt to present data for a long series of measurements, such as might be made with a given configuration and varying parameters, for example, M and R. Rather, several different configurations are investigated; these show the typical effects and their relative importance. With some of the more important effects established and the general picture thus outlined, a more detailed series of measurements can be made if required for any specific purpose.

In presenting these data, the zero of the position coordinate is taken as the (theoretical) intersection of the shock wave with the surface (e. g., see sketch in fig. 19). This is usually obtained directly from photographs by extending the straight portion of the shock wave till it intersects the surface. This gives good checks with that obtained by calculation of the wave angle, in cases where the shock wave is clean. The vertical coordinate is given as $\Delta p/p_o$, where $\Delta p = p - p_1$ and p_1 is the static pressure in the undisturbed flow ahead of the interaction; p is the local static pressure.

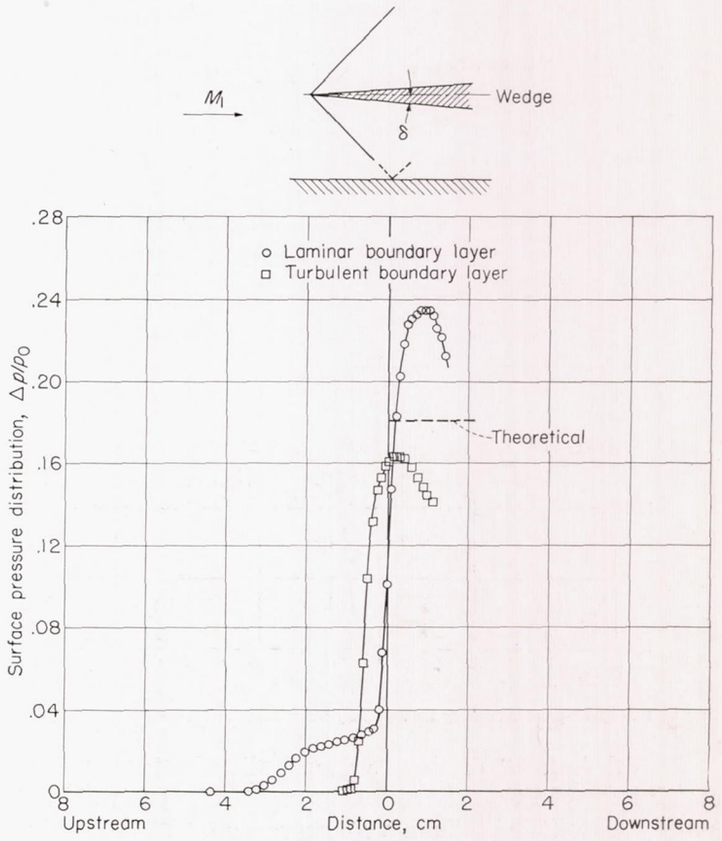

FIGURE 19.—Reflection of shock wave from flat surface. $\delta = 4.5°$; $M_1 = 1.44$; $R = 0.9 \times 10^6$.

The stagnation pressure p_o is atmospheric pressure in all cases. Reynolds number at the point of measurement and the Mach number in the undisturbed flow are also noted in each figure.

The theoretical pressure jump for the reflection, which is obtained by using figure 11 and tables of p/p_o against M, is also shown. However, the significance of this indicated theoretical pressure jump is somewhat doubtful. Slight differences in flow conditions give different effective wedge angles. In figure 19 a change of 0.01 in the theoretical value of the pressure jump would be caused by a change of 0.15° in effective wedge angle.

The pressure distributions could not be reliably continued farther downstream than shown in the figures, because of interference due to waves from the trailing edges or sides of the wedges used.

REFLECTION OF A 4.5° STEP WAVE

A pressure survey through the shock wave from a 4.5° wedge is shown in figure 20. This wave was reflected from

a flat surface with turbulent and laminar boundary layers, for which profile measurements are given in figure 17. (Also see section "Comparison of Measured and Theroretical Results.") Schlieren pictures of the reflection patterns in the two cases are reproduced in figure 16, and surface pressure distributions are given in figure 19.

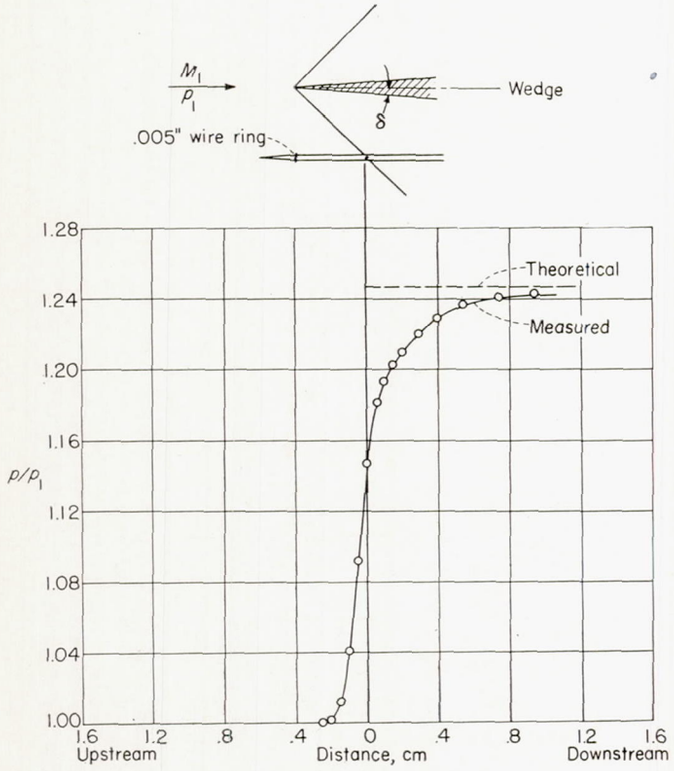

FIGURE 20.—Static-pressure survey through step wave from 4.5° wedge. $\delta=4.5°$; $M_1=1.44$.

Several features of these pressure distributions are outstanding: (1) For the turbulent case the pressure rises steeply with little preliminary compression. In the laminar case there is an initial small rise, or "bump," in the distribution, beginning considerably farther upstream of the main rise. (2) The steep parts of the curves are displaced by about ½ centimeter; for the laminar case it is farther back. (3) The pressure for the turbulent case first rises to a value near that predicted by simple theory and then decreases. In the laminar case there is an appreciable overcompression, followed by an expansion. As noted above, the indicated theoretical value is doubtful; but the difference in pressure rises for turbulent and laminar cases is real.

Figure 21 is adapted from the measurements given by Fage and Sargent (reference 11). This gives the pressure distribution due to the reflection of a wave of nearly the same strength as the one in figure 19. The figure gives data only for a turbulent boundary layer at a higher Reynolds number than that in the above case (6×10^6 as compared with 0.9×10^6), but it will be noted that the distribution is similar to the turbulent case of figure 19.

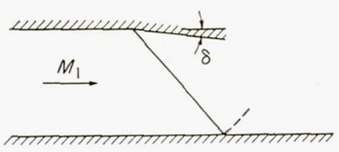

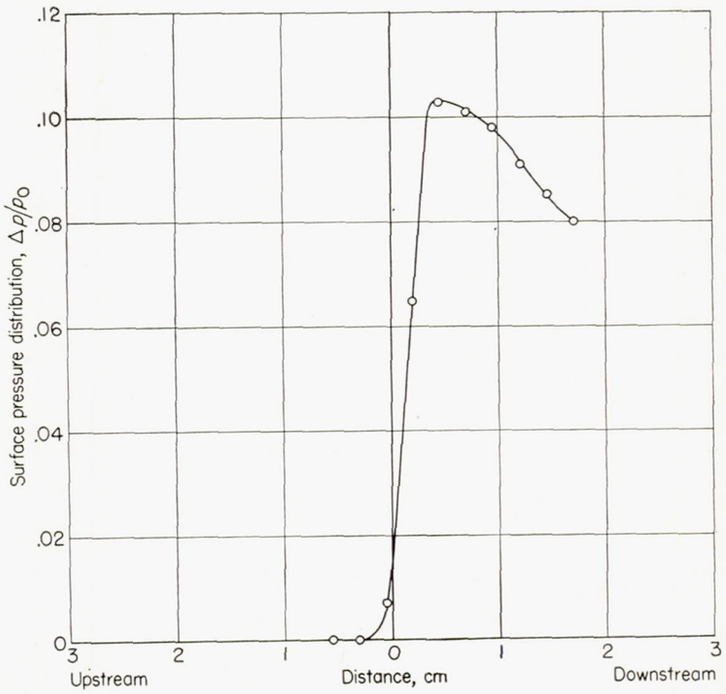

FIGURE 21.—Reflection of shock wave from flat surface (adapted from Fage and Sargent, reference 11, fig. 7). $\delta\approx5°$; $M_1=1.47$; $R=6\times10^6$; turbulent boundary layer; theoretical $\Delta p/p_o$, 0.19.

REFLECTIONS OF A 3° STEP WAVE

A similar set of measurements, using a 3° wedge, is given in figure 22. (The shock wave here is the one for which a pressure survey is given in fig. 4 ($y=2.5$ cm).) In this case, the pressure rises, in both cases, are higher than the theoretical (again note the remarks made above). The total rise in the laminar case is higher than that in the turbulent case.

MACH REFLECTIONS

Measurements of surface pressures at Mach reflections are given in figure 23. These show the same features as the regular reflections above. A schlieren picture of this Mach reflection is reproduced in figure 13 (c).

REFLECTIONS OF A 10° CONE WAVE

Figure 24 gives surface pressure distributions for the reflections of the wave due to a 10° cone. This figure should be compared with the pressure distributions at the reflection of a comparable step wave, shown in figure 22, and note should be taken of the similarity in upstream pressure distributions in the two cases.

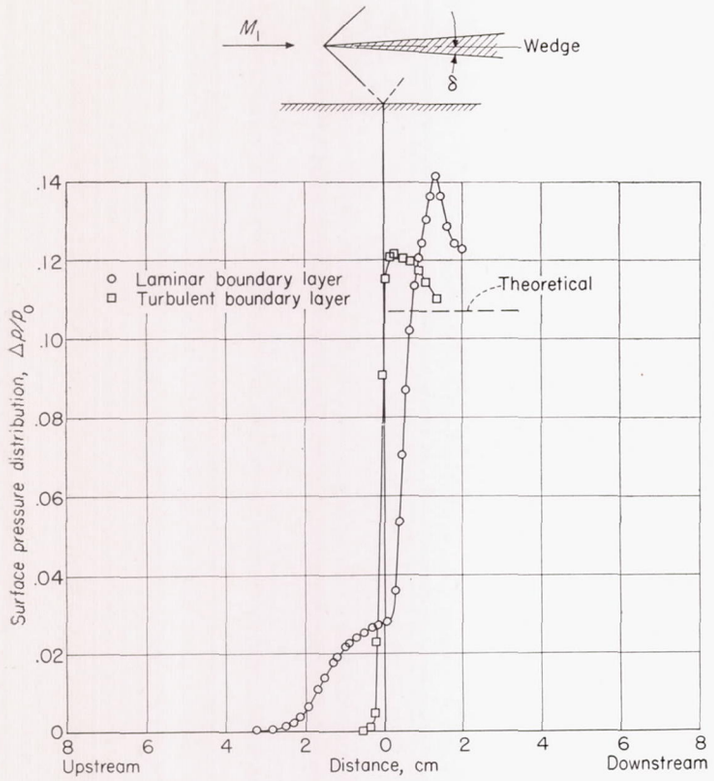

FIGURE 22.—Reflection of shock wave from flat surface. $\delta=3°$; $M_1=1.4$; $R=0.9\times10^6$.

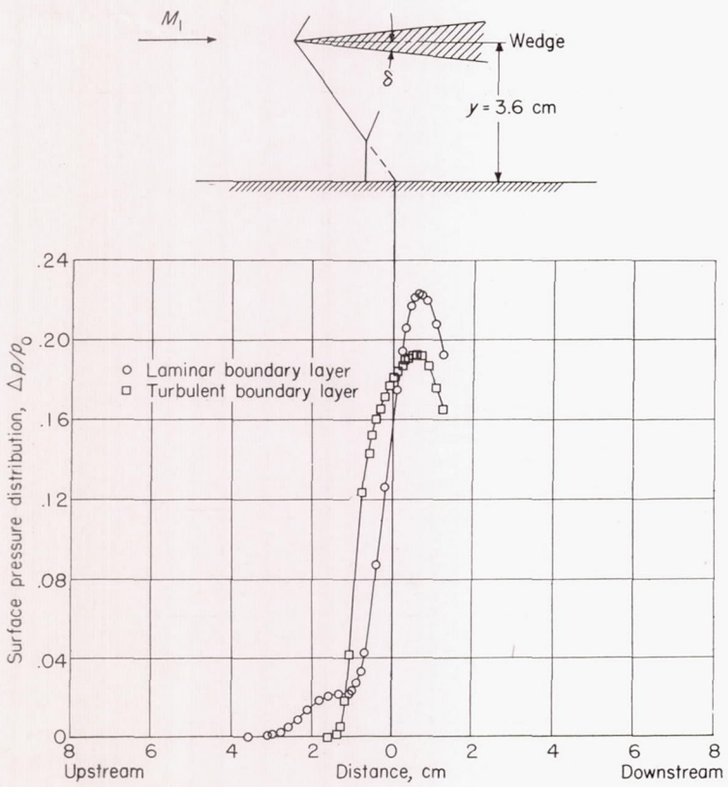

FIGURE 23.—Mach reflection. $\delta=6.5°$; $M_1=1.43$; $R=0.9\times10^6$.

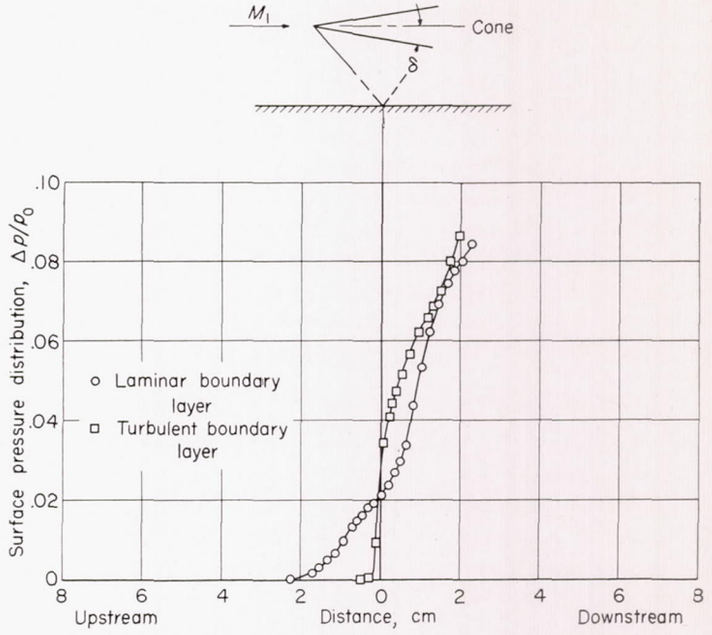

FIGURE 24.—Reflection of conical shock wave from flat surface. $\delta=10°$; $M_1=1.35$; $R=0.9\times10^6$.

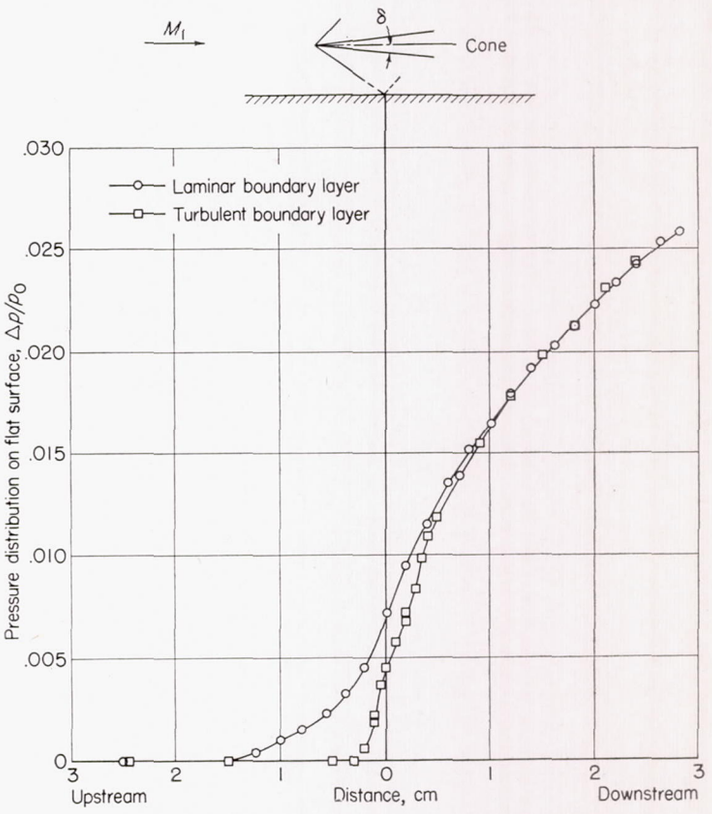

FIGURE 25.—Conical shock reflection. Half cone angle δ, 5°; $M_1=1.32$; $R=0.9\times10^6$.

REFLECTIONS OF A 5° CONE WAVE

Figure 7 gives pressure measurements through the wave, and figure 25 gives the surface-pressure measurements at the

reflections, for turbulent and laminar boundary layers. A departure from the trends of the last four cases will be observed; that is, there is no relative displacement of the two curves; they coincide with each other early.

In connection with this it should be noted that a 5° cone wave has a total theoretical pressure rise p_s/p_1 of 1.05 and corresponds, in total pressure rise, that is, in strength, to a 1° step wave. However, the initial theoretical pressure jump p_w/p_1 is only 1.002, and so, because of the effect of shock thickness, the initial pressure gradient may be only of the order 0.01 atmosphere per centimeter (see section "Remarks on Shock Waves") and separation may not occur.

SUPERSONIC FLOW AT A CORNER WITH BOUNDARY LAYER

The pressure distributions ahead of a corner, for turbulent and laminar flow, are presented in figures 26 and 27. Schlieren pictures of the two cases are reproduced in figures 3 (c) and 3 (d). The similarity between these pressure distributions and those for the reflection of an incident step wave is quite apparent.

REFLECTIONS OF IMPULSE-TYPE WAVES

An impulse-type wave was obtained in the initial part of the pressure field due to a 2° cone of 0.01-centimeter nose radius. Measurements through the wave are given in figure 6, while figure 28 gives the surface pressure distributions at reflections of the wave from turbulent and laminar boundary layers.

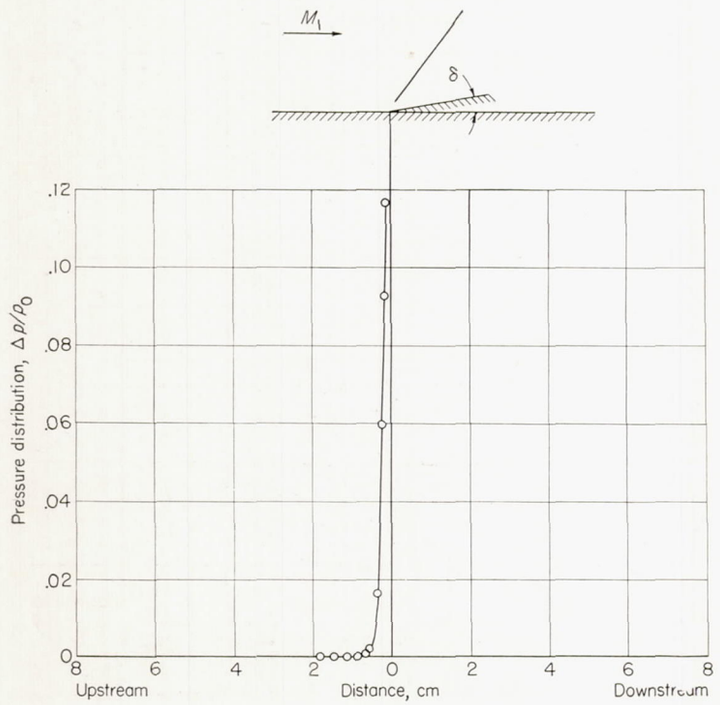

FIGURE 26.—Flow in corner. Turbulent boundary layer; corner angle δ, 10°; $M_1=1.55$; $R=0.9\times10^6$.

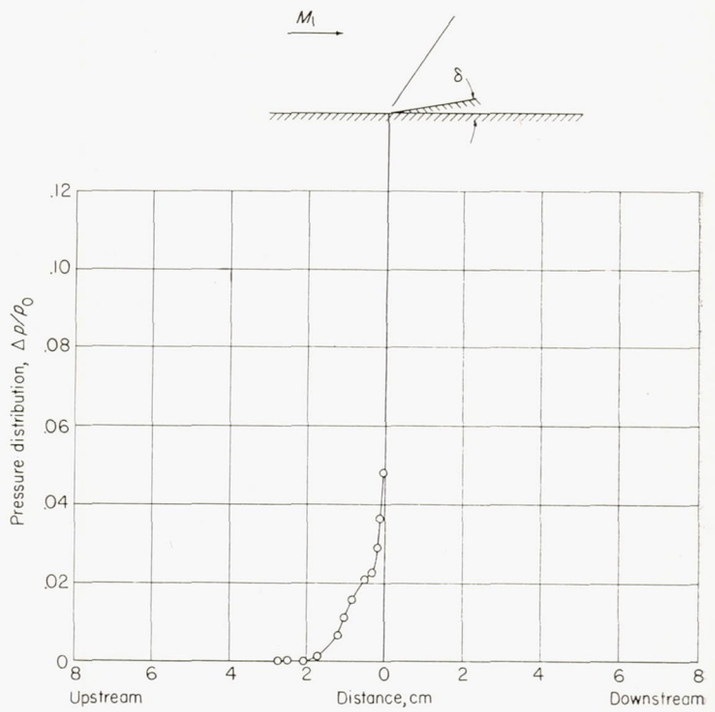

FIGURE 27.—Flow in corner. Laminar boundary layer; corner angle δ, 10°; $M_1=1.55$; $R=0.9\times10^6$.

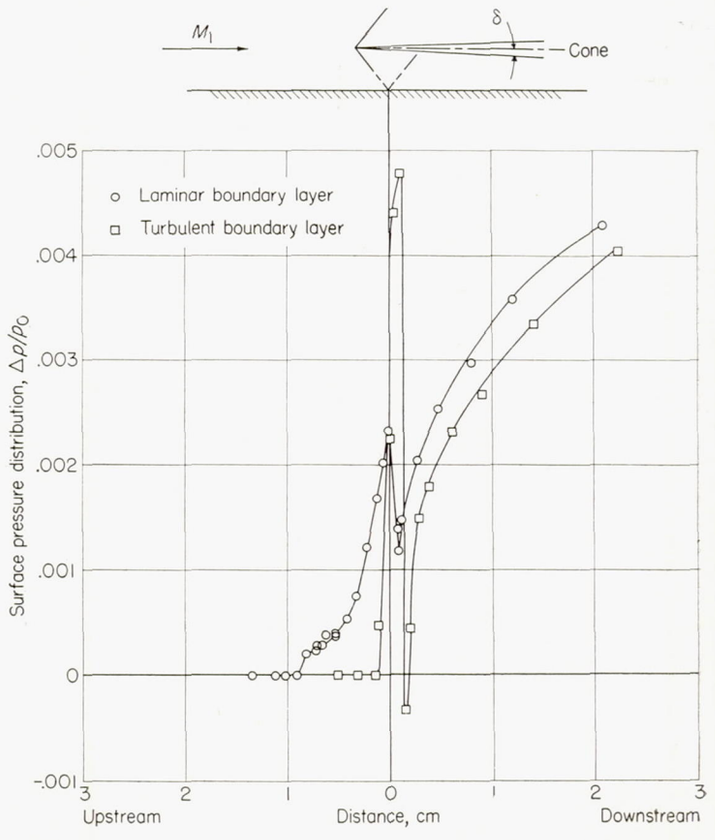

FIGURE 28.—Reflection of impulse-type wave. $M_1=1.32$; $R=0.9\times10^6$.

The upstream portions of the pressure distributions look much like the typical ones already observed above. But farther downstream the effects are different; the striking feature is the "smoothing" or "smearing" of the impulse wave by the laminar boundary layer.

In figure 29 are shown the reflections of the wave due to a 1.5° wedge. No measurements of the wave itself had been made at the time figure 29 was obtained, but it is believed to be the impulse type. The same typical smoothing by the laminar boundary layer is exhibited.

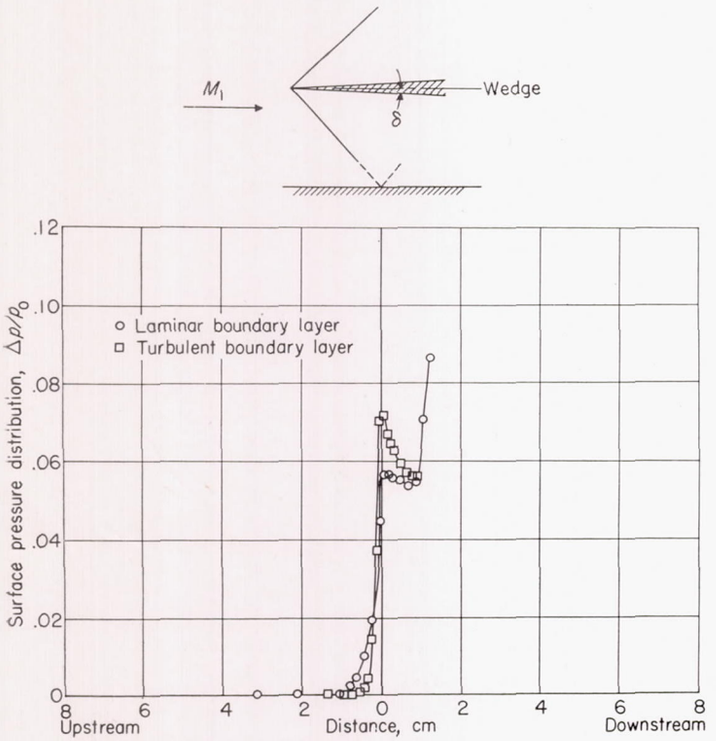

FIGURE 29.—Reflection of impulse-type shock wave from flat surface. $\delta=1.5°$; $M_1=1.43$; $R=0.9\times10^6$.

To study better the phenomena, a clean impulse-type wave (i. e., without a following compression) was obtained by the method described in the section "Remarks on Shock Waves." The form of this wave is shown by the measurements in figure 9, and schlieren pictures of the reflections from turbulent and laminar boundary layers are given in figure 30. The surface pressure distributions for the reflection are shown in figure 31. Again the smearing by the laminar boundary layer is strikingly exhibited. Note should be taken that the upstream effect is the same as that for step waves.

MODELS OF TYPICAL REFLECTIONS

The case of the 4.5° step wave was selected for further investigation in order to get a better understanding of the interaction region. Measurements of total head near the surface in the interaction region were obtained by the method described in the section "Measurements of Total Head." The measurements are given in figures 32 and 33. For a better appreciation of these total-head measurements, the static-pressure measurements of figure 19 are also partly reproduced in the same figures, this time in terms of actual pressure. The curves clearly show the thickening of the boundary layer upstream of the shock and a definite region of separation in the laminar case. (A longitudinal total-head survey in the undisturbed boundary layer very near the plate is given, in fig. 15, for comparison.)

Figure 34 is a diagram of the shock-interaction region at a turbulent boundary layer and figure 35 is that for a laminar boundary layer. These were constructed on the basis of information from the schlieren pictures (fig. 16), surface-pressure measurements (fig. 19), and total-head measurements (figs. 32 and 33). The streamline ahead of the shock in the laminar case was computed by approximating the initial pressure rise by two straight lines. The Mach numbers, other than the initial Mach number, were computed.

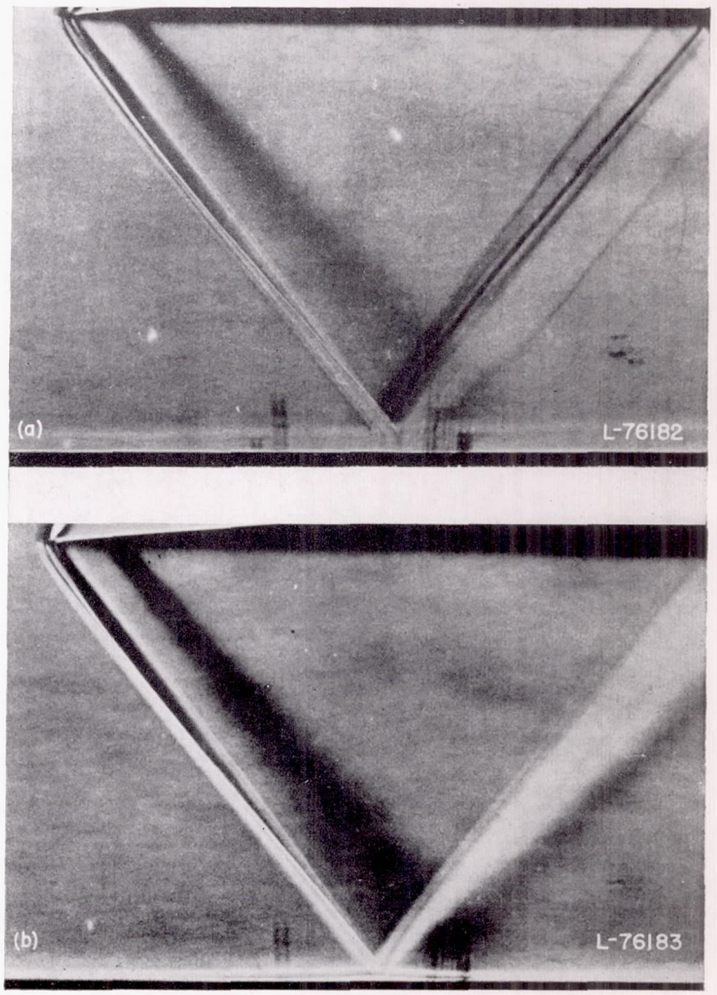

(a) Turbulent boundary layer.
(b) Laminar boundary layer.

FIGURE 30.—Reflection patterns of impulse-type wave. $M_1=1.38$.

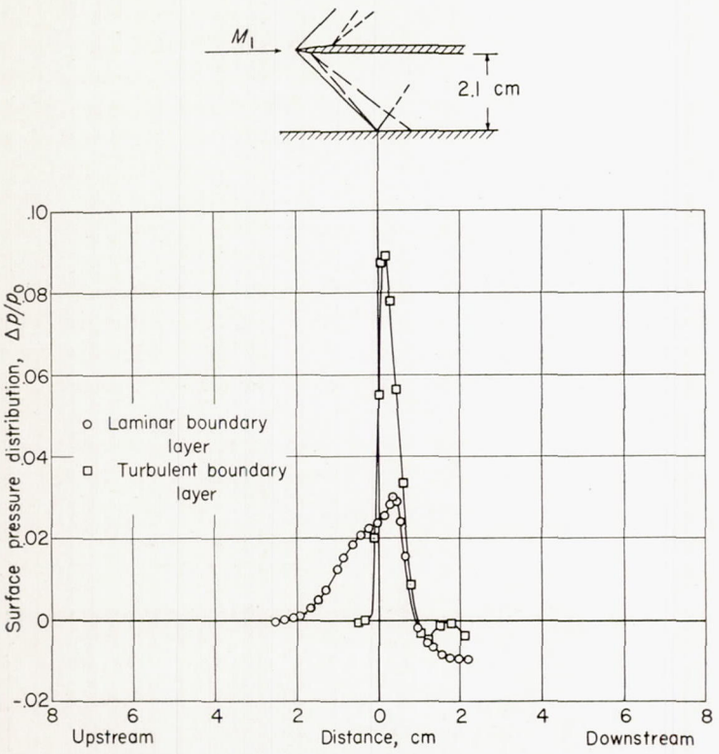

FIGURE 31.—Reflection of impulse-type wave from flat surface. $M_1=1.38$; $R=0.9\times10^6$.

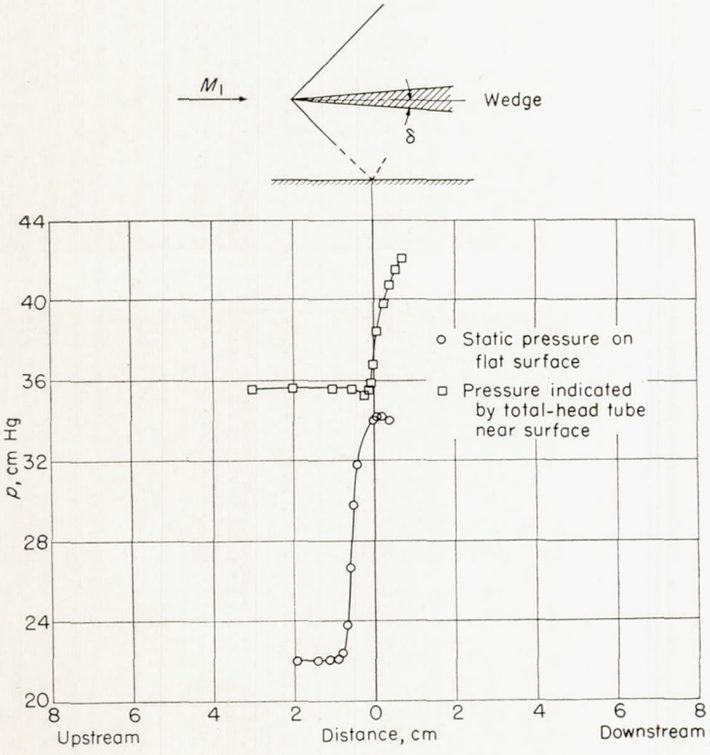

FIGURE 32.—Reflection of shock wave from flat surface. Conditions near surface with turbulent boundary layer; $\delta=4.5°$; $M_1=1.44$; $R=0.9\times10^6$.

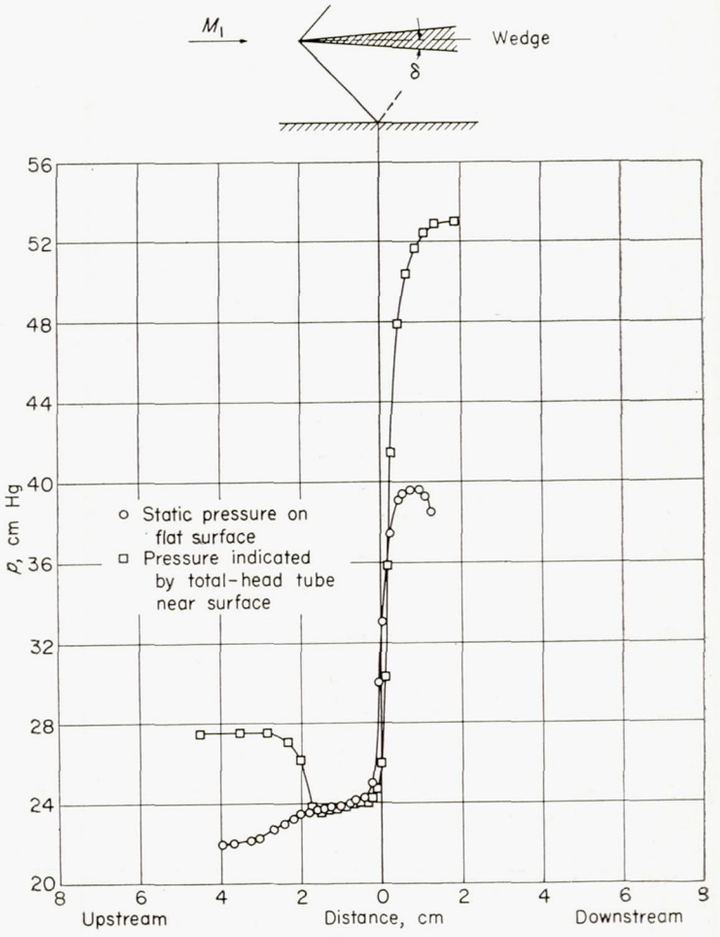

FIGURE 33.—Reflection of shock wave from flat surface. Conditions near surface with laminar boundary layer; $\delta=4.5°$; $M_1=1.44$; $R=0.9\times10^6$.

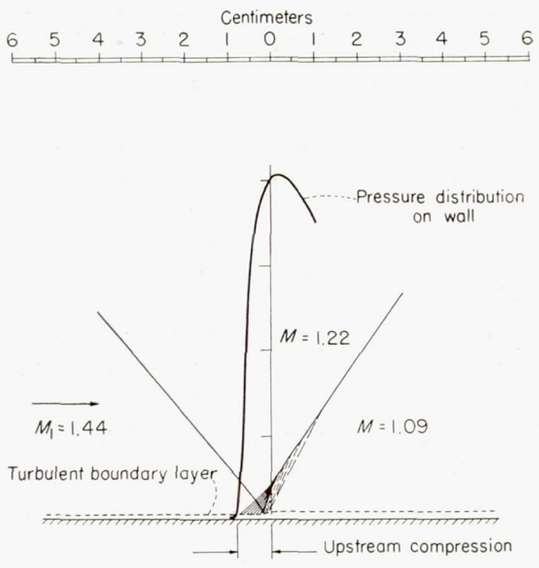

FIGURE 34.—Model of shock-wave reflection from flat surface with turbulent boundary layer. Incident wave δ, 4.5°; $M_1=1.44$; $R=0.9\times10^6$.

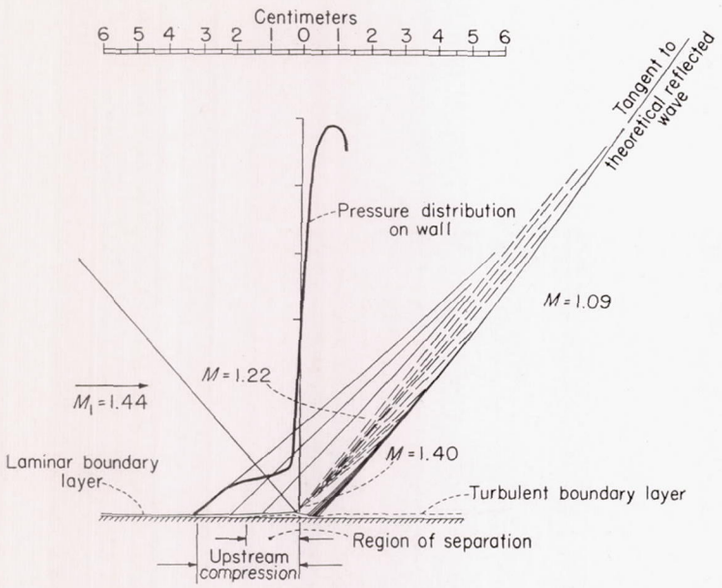

FIGURE 35.—Model of shock-wave reflection from flat surface with laminar boundary layer. Incident wave δ, 4.5°; $M_1=1.44$; $R=0.9\times10^6$.

The streamline curvature immediately following the corner (fig. 35) is of the correct order of magnitude to account for the difference in maximum surface pressures in the laminar and turbulent cases. The shape shown for the separated region is not meant to be an accurate representation. Only its extent along the flat surface is definite. The wave angle of the reflected wave far from the interaction region has been drawn, in the large, at the theoretical value. (See section "Reflection of Inclined Shock Wave from Plane Surface.")

REFLECTION OF SHOCK WAVES FROM SHEAR LAYERS

Since accurate quantitative results for reflection of shock waves from shear layers could not be obtained, only a few representative cases are discussed here. Figure 36 shows typical interaction configurations used in the attempted study of the reflection process. The incident wave from the wedge interacting with the shear layer (wake of a flat plate, 1/16 in. thick, 1½ in. long) splits up into the transmitted and reflected systems of waves. The general character of the shear layer is shown by the typical profiles, measured with a total-head tube, which are reproduced in figure 37. The widening of the wake, together with the nonuniformity of flow introduced by the trailing-edge shock waves, rendered attempts at quantitative measurements of the reflected and transmitted wave systems extremely difficult. Qualitatively, the effect of the shear-layer profile shape on the reflection process may be seen from figures 36 (a) and 36 (b) where the reflected wave is seen to be stronger when the reflection takes place from the part of a shear layer with a greater gradient and greater change in Mach number. Another point of interest to be noticed in the above-mentioned photographs is the deflection of the shear layer at the interaction. Here, again, accurate quantitative measurements proved unsuccessful. The complications mentioned above were felt to outweigh the theoretical advantages to be obtained by preliminary investigations of purely supersonic shear layers.

REMARKS ON BOUNDARY LAYERS IN SUPERSONIC FLOW

In these experiments it was necessary to have control of the boundary layer, that is, to have means of establishing laminar or turbulent boundary layers as required and of ascertaining that clean conditions in the respective cases had been obtained.

LAMINAR BOUNDARY LAYER

To obtain a surface with a laminar boundary layer a wedge-shaped plate, like that on the left in sketch (n), was used. A laminar boundary layer extending back at least 12 centimeters ($R=1.3\times10^6$) on the upper surface could be obtained. It was found best to have the upper surface at a slight negative angle of attack (about 0.1°). The leading edge must be free of nicks and other imperfections. Trials with a flat plate having a pointed nose as on the right in sketch (n) proved unsuccessful for establishing a large enough region with laminar boundary layer.

It appears that leading-edge conditions (imperfections, position of stagnation points, expansion regions, etc.) are of great importance; a systematic study of the problem has not yet been made.

In shock-wave and boundary-layer interaction, difficulties were encountered in the measurement of pressure distributions when the reflection process took place on the laminar boundary layer near the leading edge of the plate (i. e., at low Reynolds numbers). Here the upstream influence was sometimes large enough to affect the flow at the nose of the plate; this in turn affected the character of the boundary layer and the resulting interaction was even more complicated than usual. This consideration makes it imperative that the laminar regions extend sufficiently far downstream of the leading edge.

TURBULENT BOUNDARY LAYER

The production of a turbulent boundary layer requires just as much care as that of a laminar boundary layer. In subsonic flow, the transition from laminar to turbulent boundary layer depends on Reynolds number and on the amplitude (and frequency) of disturbances imposed on the laminar flow. These same parameters are important in supersonic flow, but no quantitative data are available. As already mentioned above, nose shape, position of stagnation point, leading-edge imperfections, and so forth appear to influence strongly the transition.

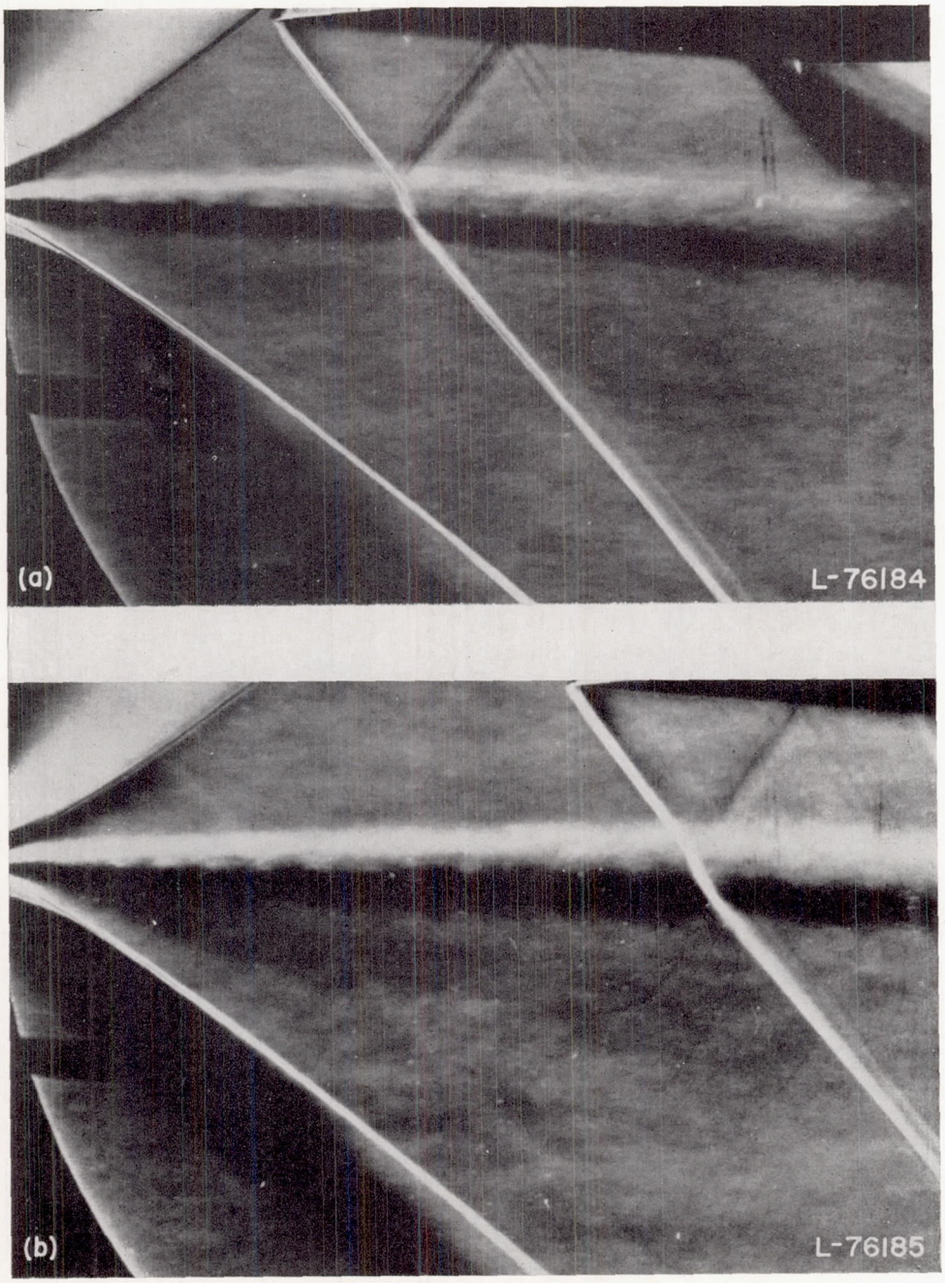

(a) Reflection 3 centimeters behind trailing edge.
(b) Reflection 5 centimeters behind trailing edge.

FIGURE 36.—Typical reflections of shock wave from shear layer. $M=1.36$; incident wave δ, 4.5°; scale, two and one-half times full scale.

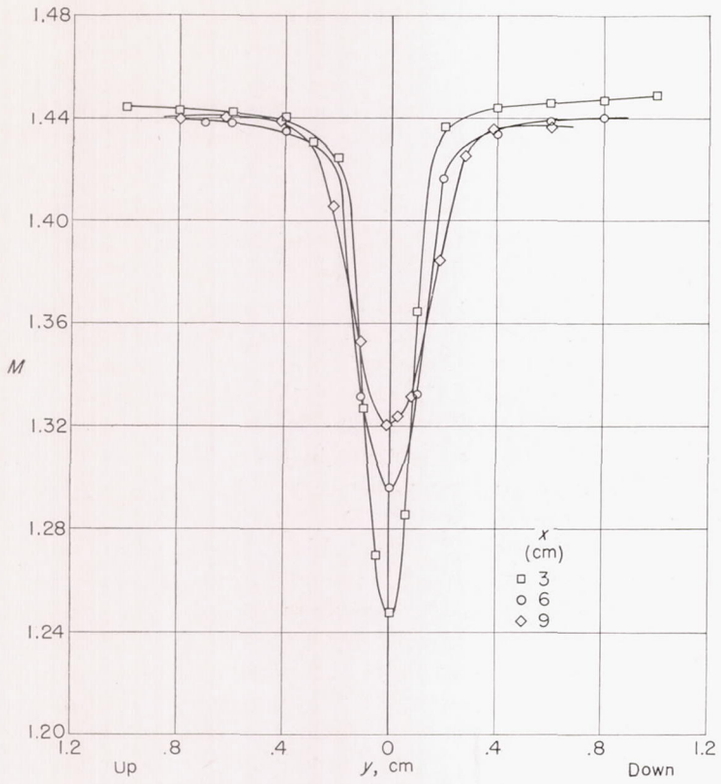

FIGURE 37.—Typical Mach number profiles in wake of flat plate. x, distance behind trailing edge; y, distance from center line of wake.

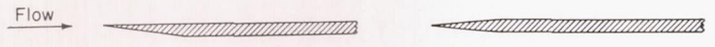

(n) Cross sections through plates.

Tracings of the transition region, on the surface of the plate shown on the left in sketch (n), were obtained by the technique described in the section "Visualization of Transition in Boundary Layers." These tracings are reproduced in figure 18. Turbulence is established early in the flow directly behind nicks in the leading edge and spreads out into wedge-shaped zones, by the process of contamination (reference 18). Removal of the nicks from the leading edge and careful smoothing eliminate the wedge-shaped turbulent regions from the middle of the plate but not the regions on the sides, which originate at the juncture of plate and side walls. (These turbulent zones must be taken into account in any laminar-boundary-layer measurements which give an integrated value across the span of the plate, e. g., by quantitative schlieren, interferometer, or X-ray techniques. Such turbulent side regions, and any other mixed regions that might exist on the middle of the plate, will introduce considerable errors if neglected in the calculations.)

The above discussion indicates that it may be difficult to obtain a clean turbulent boundary layer, unless regions well downstream of the leading edge are used (more than about 15 cm in the present case). Even raising R is not sufficient to ensure that there may not be long "tongues" of laminar flow extending into the turbulent region. In the present experiments it was found convenient to ensure an early well-developed turbulent boundary layer by stretching a 0.005-inch wire across the surface of the plate, about an inch downstream of the leading edge. This creates a disturbance in the laminar boundary layer which causes an early transition to a uniform turbulent flow (fig. 18 (c)).

IDENTIFICATION OF LAMINAR AND TURBULENT BOUNDARY LAYERS

In schlieren or shadow pictures, the laminar boundary layer has a sharply defined edge, while the turbulent boundary layer is thick and diffuse (cf. figs. 12 (b) and 12 (a)). At some distance downstream of the leading edge, where the turbulent side regions have become fairly wide, and in cases where mixed regions exist at the middle of the plate, this method will be confusing. However, when it is supplemented by other checks, for example, study of transition zones and measurement of profiles, so that the typical appearances are correctly learned, then the visual method can be reliable and very convenient.

Figure 17 shows typical profile measurements in laminar and turbulent boundary layers established by the methods discussed above. They were obtained from total-head measurements and calculated on the basis of a Prandtl number of unity. Since the profiles are principally for comparison, it was not necessary to make more elaborate measurements and calculations.

It will be noted that in these experiments the boundary layers are laminar or turbulent at the same Reynolds number. Doubt is sometimes expressed as to whether the distinction is valid, that is, whether an "artificial" production of turbulent boundary layer, as by the wire technique described, gives a "genuinely turbulent" boundary layer. In this connection it should be recalled that in all cases the production of turbulent boundary layer is artificial. That is, the establishment of a turbulent boundary layer is a transition from an essentially unstable to a stable configuration. The transition can take place over a wide range of Reynolds numbers depending on the disturbances imposed on the (unstable) laminar flow. Turbulent flow produced by early transition is just as genuinely turbulent as that developing later and shows the same characteristics (cf. figs. 19 and 21).

SUBSONIC SUBLAYER

In some theoretical investigations of shock-wave and boundary-layer interaction (cf. reference 13) the thickness

of the subsonic part of a boundary layer is important. It will be noted in figure 17 that there is little difference in subsonic thicknesses of the laminar and turbulent boundary layers, at least in that case. Furthermore, it is obvious that in the cases where the outer flow is near $M=1$, for example, transonic flow, there could be little difference in subsonic thicknesses. Reference 6 gives measurements demonstrating such a case.

COMPARISON OF MEASURED AND THEORETICAL RESULTS

Some discussion concerning the production of shock waves in the presence of walls with boundary layer and of possible reflection patterns has already been given. A few words may be added here on the comparison of the measured results with the existing theoretical studies of Howarth, Tsien and Finston, Marble, and Lees. Howarth (reference 14) deals with the case of an impulse-type shock wave in a uniform supersonic field which is reflected from a half-infinite subsonic field. The problem is then characterized by two Mach numbers M_1 and M_2 in the supersonic and subsonic half plane, respectively, by the strength of the wave, and finally by the only characteristic length of the problem, the width ϵ of the impulse-type wave. Howarth uses the standard linearized potential equation and discusses the pressure distribution near the discontinuity surface as a function of M_1 and M_2 which occur only in a combination k

$$k=\frac{\gamma_2 M_2^2\sqrt{M_1^2-1}}{\gamma_1 M_1^2\sqrt{1-M_2^2}}$$

Thus k represents a reflection coefficient. On the basis of this model, Howarth is able to demonstrate quantitatively in a simple fashion the upstream influence and, in general, the pressure distribution produced by the incoming compression wave; both compression and expansion regions appear in this distribution.

Tsien and Finston (reference 13) have attempted to improve Howarth's model to make it more closely correspond to the boundary-layer problem. They retain the linearization but consider the subsonic part of Howarth's model to be bounded by a solid surface. Thus a new length b, the thickness of the subsonic region, enters. On the basis of this model, which is now characterized mainly by M_1, M_2, and b, two cases are discussed: The reflection of a step wave and the flow near a small corner. Pressure distributions on the wall and near the surface of discontinuity are obtained. The combination of compression and expansion in the reflected wave is again obtained and the upstream influence is demonstrated in the case of both the reflection and the flow within a corner. The authors then proceed to discuss the experimental results, specifically the difference in the interaction process between laminar and turbulent boundary layers, and arrive at the conclusion that the thickness of the subsonic part of a boundary layer is the characteristic length parameter and that this length is of a different order of magnitude in the laminar and turbulent layers. It has already been pointed out that in all cases so far investigated the subsonic sublayer is of roughly the same thickness in the laminar and turbulent layers, and hence the argument of Tsien and Finston is certainly not correct.

The subsonic sublayer is of major importance and one is a priori tempted to define a length parameter based on this thickness b and the Prandtl-Glauert factor $\sqrt{1-M_2^2}$, but one difficulty is immediately apparent, namely, that M_2 in an actual case is indefinite since $\sqrt{1-M_2^2}$ varies from 0 to 1 in the subsonic layer. Hence a certain mean value for M_2 should be taken which would be different in the laminar and turbulent cases. The obvious difficulty of determining this mean value in a rational way led, as a matter of fact, to Cole's investigation of the propagation of sound waves in a boundary layer briefly mentioned in reference 6. Here the diffraction of sound waves due to the velocity profile was studied and the difference between laminar and turbulent profiles was shown.

Marble (reference 12) restricts himself to the case of purely supersonic flow and considers the reflection and transmission of weak shock waves through shear layers. The omission of the subsonic part is evidently a very great simplification of the problem and excludes the possibility of comparing Marble's results with boundary-layer processes. However, this simplification enables Marble to consider arbitrary velocity distributions. The discussion of various reflection patterns as given by Marble is rather interesting and important for the outer layers of a boundary layer where his computations apply locally.

The three papers discussed above have in common that the equations are linearized. Actually the attempts made and discussed in this report to investigate a typical shear layer for a comparison with Marble's theory were essentially intended to check on the applicability of the linearization since this is the only stringent assumption in Marble's work. In the case of a shear layer the linearization appears to apply reasonably well. In the boundary-layer investigation, on the other hand, the measurements showed that the interaction process is nonlinear in character even for very weak waves, that is, for waves for which the linearized theory of supersonic flow (e. g., for airfoils) is known to hold well. As a matter of fact, in the measurements reported here it was difficult indeed to obtain reflections from a laminar boundary layer without local separation.

Lees (reference 9) has extended and used a procedure, given independently in reference 8, in which the Pohlhausen method is used together with simple supersonic-flow theory of the outer flow to account for the nonlinear interaction process. This attempt appears to be at present the most realistic one, since the measurements clearly indicate that the behavior of the boundary layer in a pressure gradient ahead of the shock wave is of primary importance. In agreement with the experimental results reported here, Lees finds that the laminar boundary layer should almost always separate in a shock-wave reflection process. Still, Lees' model and assumptions are too restrictive to lead to quantitative results as yet, and the validity of the procedure, especially since separation occurs, is not certain.

The problem of computing the length of upstream influence, if the shock-wave and boundary-layer characteristics are known, has so far not been solved quantitatively.

CONCLUSIONS

From an investigation of the reflection of shock waves from boundary layers, the following conclusions are drawn:

1. If an oblique shock wave is reflected from a solid surface in steady flow, then the reflected wave pattern depends strongly upon the state of the boundary layer on the surface. Laminar and turbulent boundary layers lead to very different reflection patterns in the neighborhood of the surface. The region in which the differences are marked extends to several hundred boundary-layer thicknesses out from the solid surface. The reflection in the turbulent case is much closer to the nonviscous idealization. In the laminar case the reflection process differs essentially from the nonviscous pattern.

2. The laminar boundary layer almost always separates in a limited region ahead of the impinging shock wave. The pressure increase extends upstream for distances of about 50 boundary-layer thicknesses in the Mach number and Reynolds number range investigated. In spite of the local separation and the pressure gradient, transition does not always occur immediately following the reflection process. In the turbulent boundary layer no separation was found.

3. Similar results hold for the interaction with a shock wave originating in a corner. The pressure distributions here are similar to those found in the reflection pattern; in the laminar case the influence of the corner extends far upstream.

4. Shock waves of the step type have to be distinguished from the impulse-type wave. An impulse-type wave consists of a shock followed immediately by an expansion wave. An impulse-type wave can be produced by a suitable leading-edge shape on a wedge. Impulse-type waves are found also to originate from wedges and cones of small deflection angle. Here nose curvature and viscous effects are the primary causes for the occurrence of the impulse wave.

5. The essential feature in boundary-layer interaction is the behavior of the boundary-layer flow in the region of pressure gradient upstream of the shock wave. Laminar and turbulent layers differ in this respect and not mainly in the thickness of the subsonic sublayer.

6. The laminar boundary layer on a flat plate in supersonic flow shows wedge-shaped transition regions originating from the side walls and disturbances of the surface, similar to the well-known subsonic case. This contamination effect is important for the evaluation of boundary-layer profiles from interferograms and, in general, for all methods in which measurements taken in the boundary layer are integrated across the tunnel.

California Institute of Technology,
Pasadena, Calif., *August 16, 1949.*

APPENDIX

CALIBRATION AND EVALUATION OF FLEXIBLE NOZZLE

INTRODUCTION

The problem of using a flexible nozzle for the production of continuously variable, shock-free, uniform, supersonic flow consists essentially in devising a means of closely approximating the requisite aerodynamic shapes by the deflection patterns of the nozzle plate. An analytical attempt at determining the optimum end conditions, positioning of loading points, and magnitude of the loadings may, in general, be set up as a beam problem with known end conditions of the beam (direction usually fixed, for smooth entrance and exit flow conditions) and point loads. The control variables would then be the number, the location, and the magnitude of the loads. The aim is to reproduce prescribed shapes over a part of the span. In order that the representation as a beam be a reasonable one the stiffness ratio of the nozzle plate must be high.

BRIEF DESCRIPTION OF TEST SECTION INCORPORATING FLEXIBLE NOZZLE[7]

The working section of the GALCIT 4- by 10-inch transonic tunnel is sketched in figure 14 showing the essential features of the design. The floor block of the test section carries the one-wall flexible nozzle plate together with the swivelling jack-screw controls for the main nozzle and the second throat.[8] The floor is hinged just downstream of the main jack and its downstream end can be raised or lowered by a jack at the exit end to alter boundary-layer compensation. The alterations in boundary-layer allowance can be carried out during operation. The ceiling block of the tunnel supports the entire traversing mechanism and contains a slot for the traversing arm. A pressure box mounted on the ceiling block encloses the traversing mechanism and seals it to the test section. Pressure sealing of the test section is secured by means of rubber tube-in-groove seals between the side walls and floor and the ceiling blocks. The main flexible nozzle consists of a spring steel plate of varying thickness as shown in figure 38. It is anchored in the contraction, with the downstream end also direction-fixed but free to move horizontally on rollers when deflected by the jacks. The second-throat nozzle plate begins where the primary nozzle ends. The flexible second throat acts as a supersonic diffuser during supersonic operation and as a speed control for the subsonic range.

[7] A more detailed description of the design may be found in reference 12.

[8] Originally, one more control in the form of a bending-moment arm was incorporated. However, the use of this control was subsequently found to be unsatisfactory and at the present time the arm is used only for the purpose of providing an extra guide support for the plate.

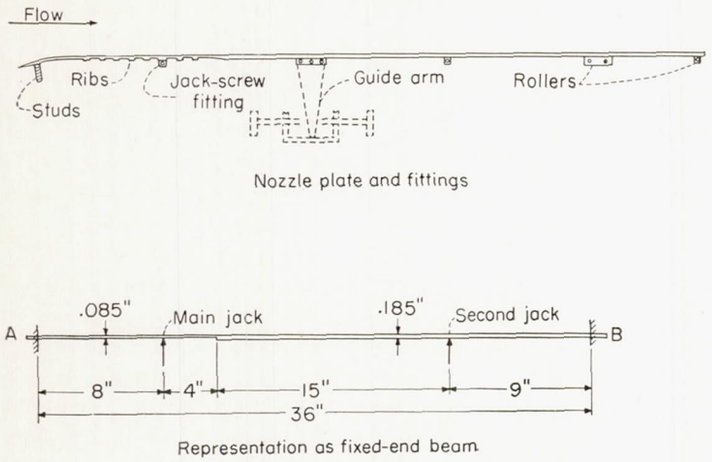

FIGURE 38.—Flexible nozzle plate.

MATCHING PROCEDURES

In the interests of a simple, practical design for the GALCIT 4- by 10-inch transonic wind tunnel (see reference 12 for details), the problem stated in the introduction to the appendix was further narrowed down. Some of the less important variables were eliminated by physical considerations of design and trial-and-error methods. The number of jack points, or loads, on the plate was restricted to two. The location of these was fixed. Figure 38 shows the final configuration adopted for the flexible nozzle plate. This procedure was justified later by tests (reference 12, p. 14) which showed that, with the nozzle controls set to reproduce approximately the design aerodynamic shapes, the flow in the test section was reasonably uniform. For an easy, continuous operation of the tunnel it was necessary to be able rapidly to set the control jacks for wave-free flow at any desired Mach number in the design range. It was logical to determine the settings by systematic calculation rather than to obtain a purely experimental calibration. For this purpose, the simplified problem may be posed as follows: Given a beam of known thickness distribution with direction-fixed ends and loaded at two specific locations with point loads W_1 and W_2, it is required to find a combination of W_1 and W_2 producing a deflection shape of the beam closely matching a given curve (the required aerodynamic shape) and at the same time attaining a prescribed maximum deflection. This restriction on the maximum of the deflection curve arises out of the unique area ratio (test section to throat section) associated with a desired supercritical flow in the test section. The known dimensions and end conditions of the nozzle plate are sufficient to define a systematic procedure for determining the jack positions in order that the nozzle plate shape may approximate prescribed shapes (reference 19). In particular, this knowledge permits a chart of possible plate shapes with a given maximum to be drawn with the load ratio $W_2/W_1=\nu$ as a parameter. Such a chart is shown in figure 39. The value of ν, designating the shape which best fits the aerodynamic curve, has to be determined from an observation [9] of figure

[9] This graphical process of matching has to be adopted in preference to a purely analytical procedure for two reasons: (a) Rapid determination of the parameter ν and (b) there being only two control points, it is extremely difficult to formulate an effective and simple analytical criterion for matching. For instance, with only two control points, a fit in the sense of "least squares" is entirely inadequate. (See reference 19, p. 15.)

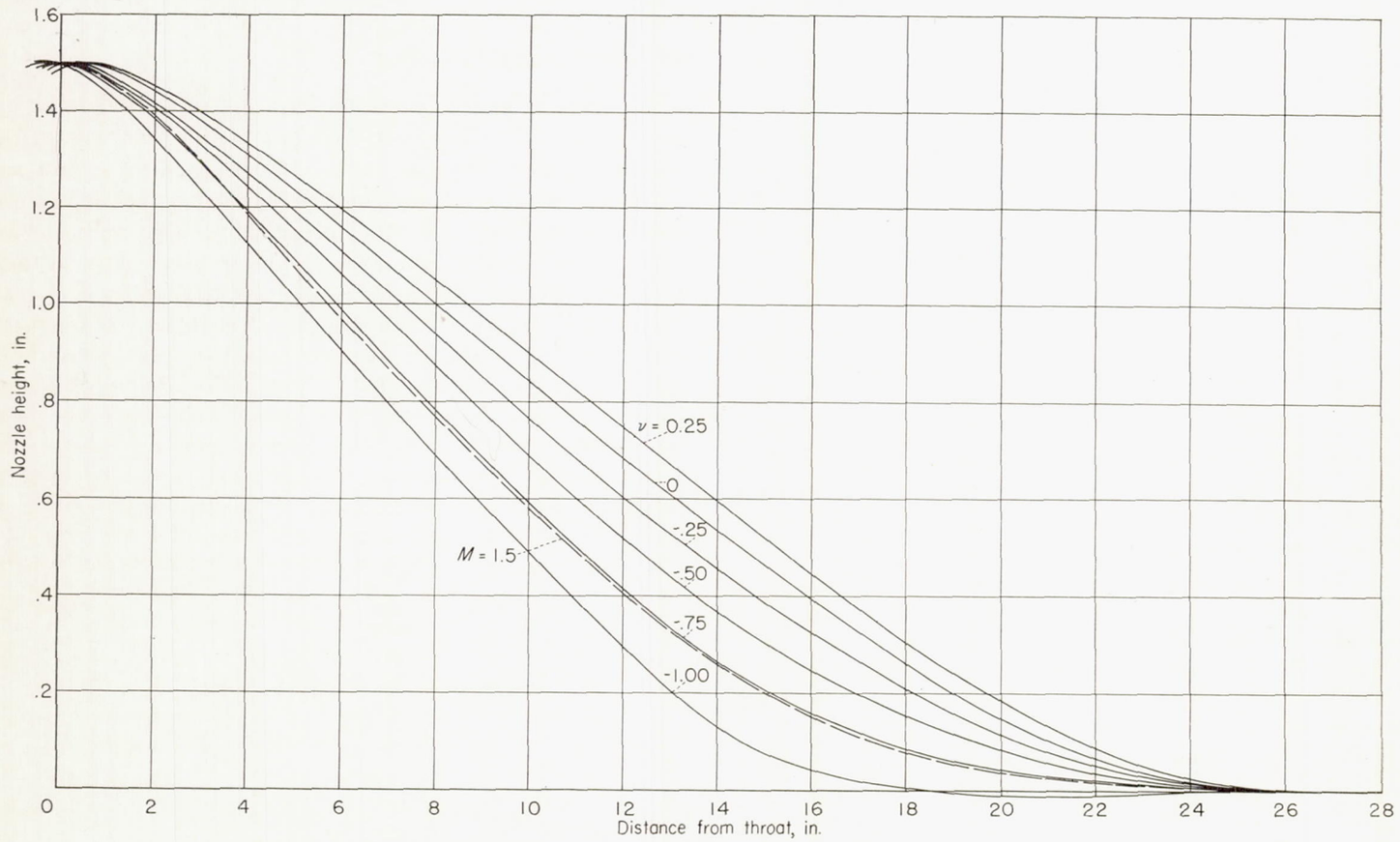

FIGURE 39.—Matching of aerodynamic and elastic shapes. $M=1.5$.

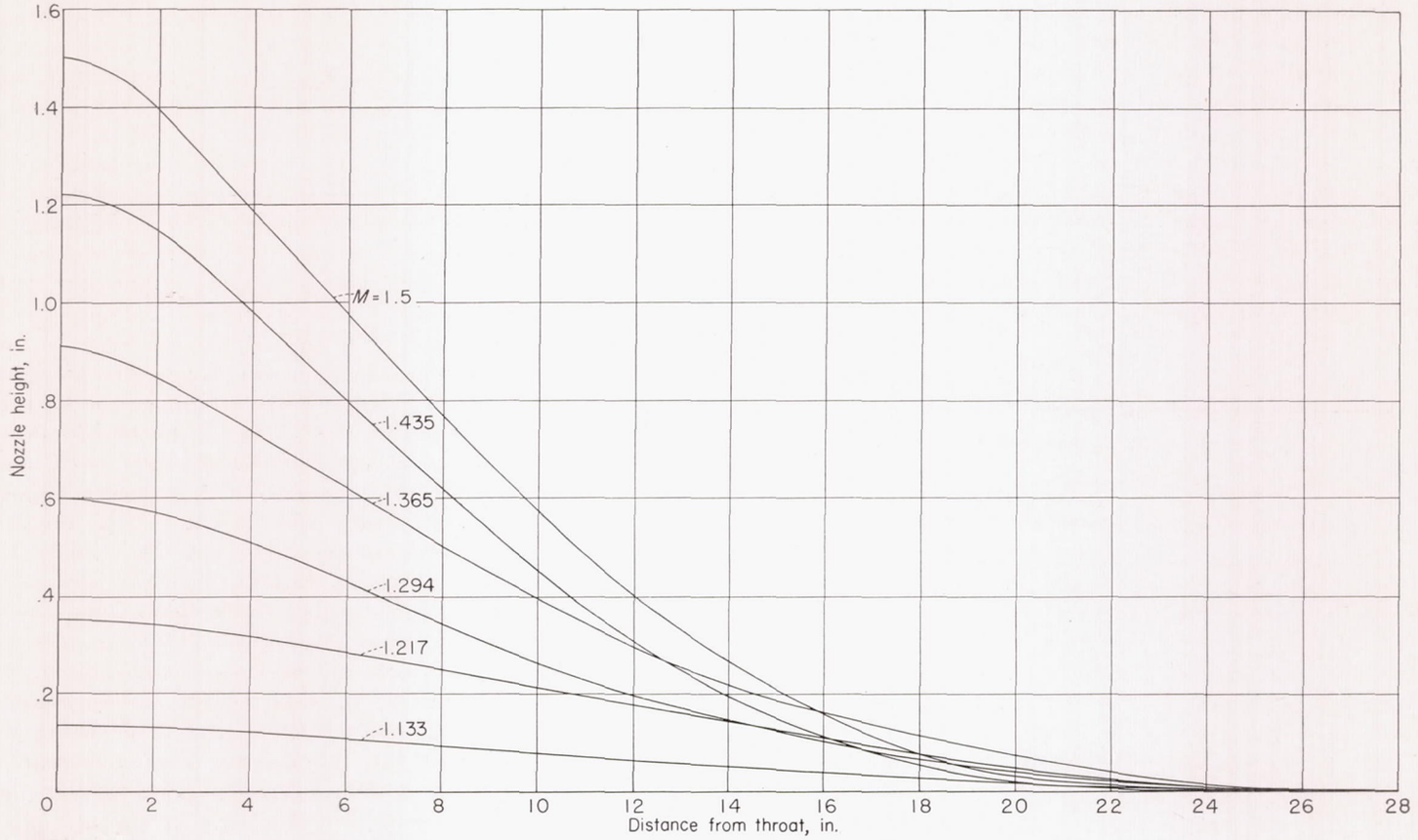

FIGURE 40.—Aerodynamic nozzle shapes. GALCIT 4- by 10-inch transonic wind tunnel.

39 superposed on the design shape (fig. 40) being approximated. The corresponding control settings are then easily computed since the deflection influence functions for the nozzle plate are known. Figure 40 shows the six aerodynamic design shapes, and a representative case of matching for determining the parameter ν is shown in figure 39. Table I shows the control settings obtained by this procedure for the operating range of the tunnel. The maximun discrepancy in ordinates, over this range, between the design shapes and the plate deflection curves is approximately 2.5 percent.

TABLE I

CONTROL SETTINGS FOR FLEXIBLE NOZZLE

M	Jack 1 (in.)	Jack 2 (in.)
1.133	0.120	0.029
1.217	.311	.088
1.294	.547	.078
1.365	.843	.089
1.435	1.121	.091
1.504	1.379	.112

CALIBRATION AND EVALUATION

A series of test-section surveys was made at the calculated control settings for the purpose of calibration of the flexible nozzle and determination of the degree of uniformity of the flow. The surveys were made by means of an 11-inch-diameter circular Duralumin plate with a row of radially located pressure holes (0.0135-in.-diam.) spaced at intervals of ½ inch. The circular plate replaced one of the glass windows in the sides of the tunnel, its center approximately coinciding with the center of the 10- by 10-inch test section.

Figures 41 and 42 show the vertical and horizontal Mach number distributions in the test section over the supersonic range of operation. The vertical distributions (fig. 41), revealing the effect of waves originating at the nozzle, indicate considerably greater uniformity of flow as compared with that shown by the horizontal surveys. The maximum variation of Mach number (from the mean) in the vertical direction over the entire operating range is approximately ± 0.5 percent as compared with ± 2.5 percent in the horizontal direction (fig. 41). The smooth vertical distributions bear out the fact that because of the use of a relatively thick, high-strength plate for the nozzle there are no local distortions in the plate. Furthermore, the plate was observed to be vibrationally very stable. The nonuniformity in the

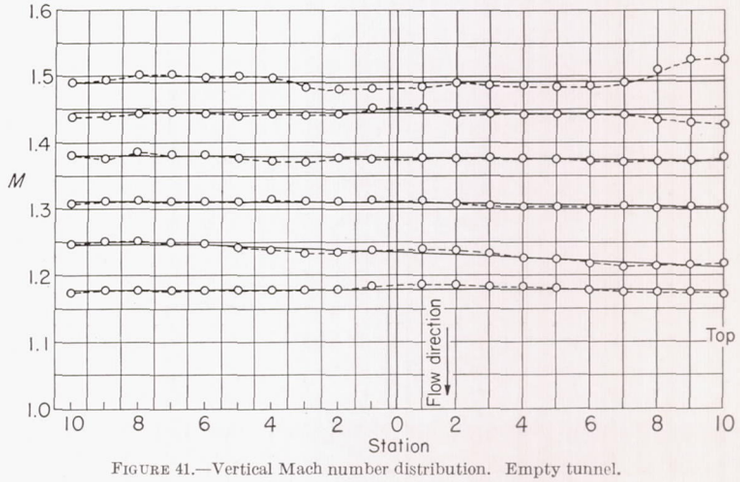

FIGURE 41.—Vertical Mach number distribution. Empty tunnel.

horizontal surveys was traced to the disturbances introduced at the joints in the sectioned side walls. Careful sealing of the joints showed that the main cause of these disturbances was slight leakage at the sections. In order to remove all doubt about the origin of the waves and, further, to ascertain the smoothest flow possible in the tunnel, the sectioned side walls were replaced by smooth, continuous panels made out of plastic-lined wood. A horizontal survey of the flow along the flow direction with these continuous side walls is shown in figure 43. The variations are now of the same order as those in the vertical surveys.

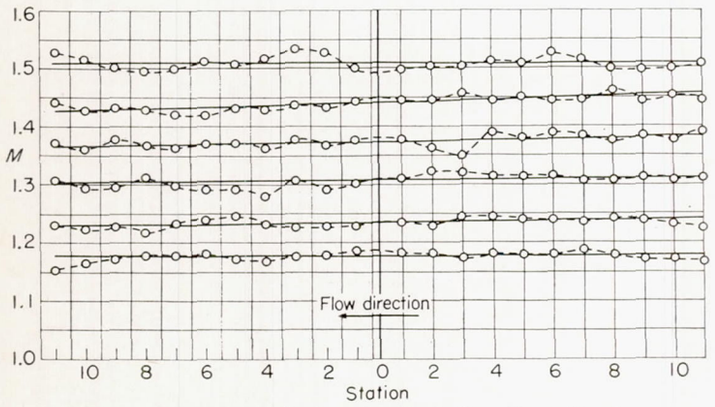

FIGURE 42.—Horizontal Mach number distribution. Empty tunnel.

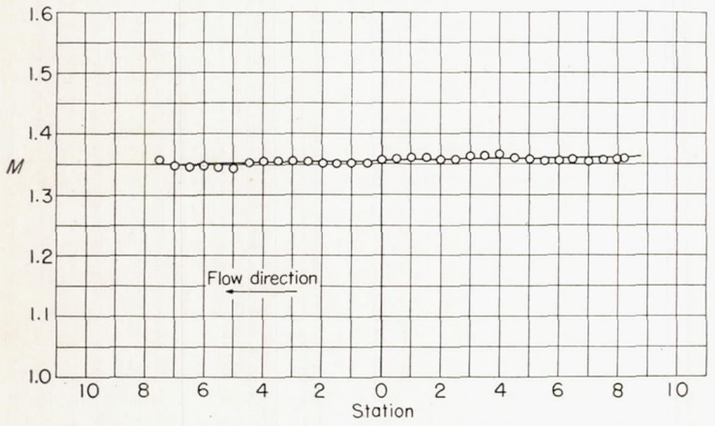

FIGURE 43.—Horizontal Mach number distribution with one-piece side walls. Empty tunnel.

FURTHER CORRECTION AND IMPROVEMENT OF FLOW

The test-section surveys presented in figures 41 and 42 were all conducted with the same boundary-layer compensation (0.021 in./in.) with the exception of the $M=1.51$ survey. As seen in these figures, the surveys reveal this compensation to be tolerably good over the working range. However, small over-all gradients do exist in the flows shown. Also the average test-section Mach numbers actually obtained differ by small amounts from those indicated by the control settings. These small discrepancies are mainly due to the inaccuracies in the boundary-layer allowance. It was found possible to minimize the over-all gradients by making small adjustments of the movable floor wall, so changing the boundary-layer compensation without appreciably affecting the shape function of the nozzle plate. Figure 44 shows test-section surveys for $M=1.5$ with different settings of the compensation. Figure 44 (a) shows the flow with the original compensation of 0.021 inch per inch while figure

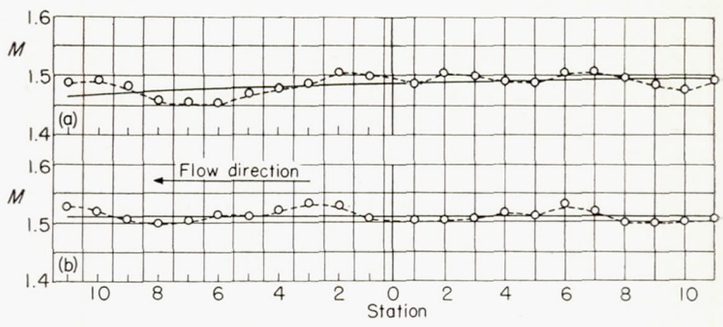

(a) Before change.
(b) After change.

FIGURE 44.—Effect of change in boundary-layer correction on horizontal Mach number distribution. $M=1.5$.

44 (b) shows the improved flow. The gradient has been effectively eliminated and the magnitude of the variations smoothened out.

The deviations of average test-section Mach number from the indicated (calculated) values are due mainly to slight differences in the area ratios. The effective area ratio, after allowance for boundary-layer growth and small deflections of the nozzle plate due to aerodynamic loading, differs from the theoretical ratio on which the nozzle control computations are based. In view of the quite smooth, uniform flow achieved at the calculated control settings, a simple correction based on the observed mean flow in the test section served to calibrate the jack controls for the production of flows with any desired Mach number. Figure 45 shows the calculated control settings corrected in this manner.

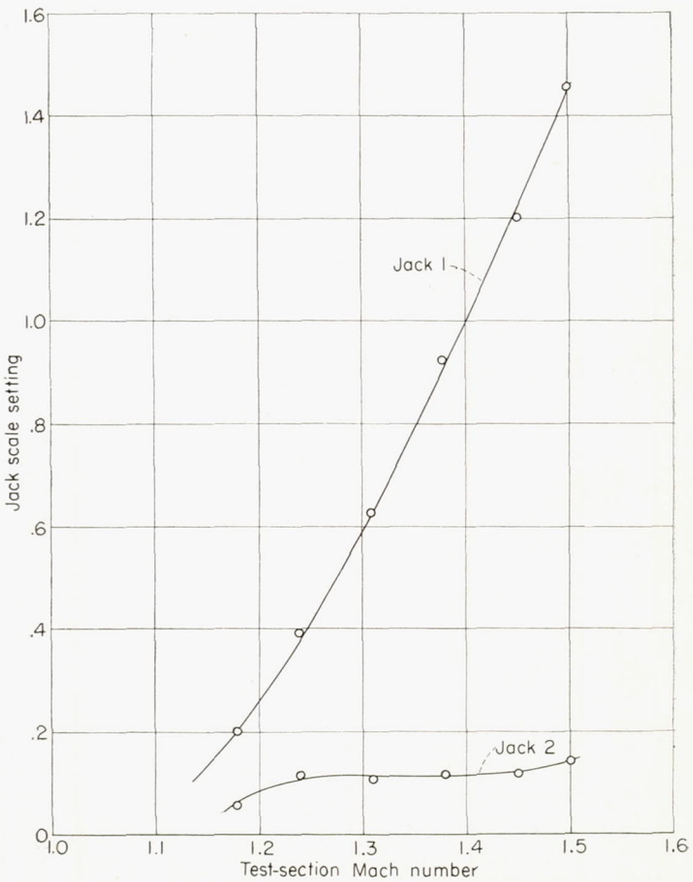

FIGURE 45.—Flexible-nozzle control settings.

SUBSONIC OPERATION

For the subsonic range of operation of the tunnel a flexible second throat is used as a speed control using the choking technique (reference 20) as a means for stabilizing the flow. Figure 46 shows the calibration curve for the speed control for the subsonic speed range.

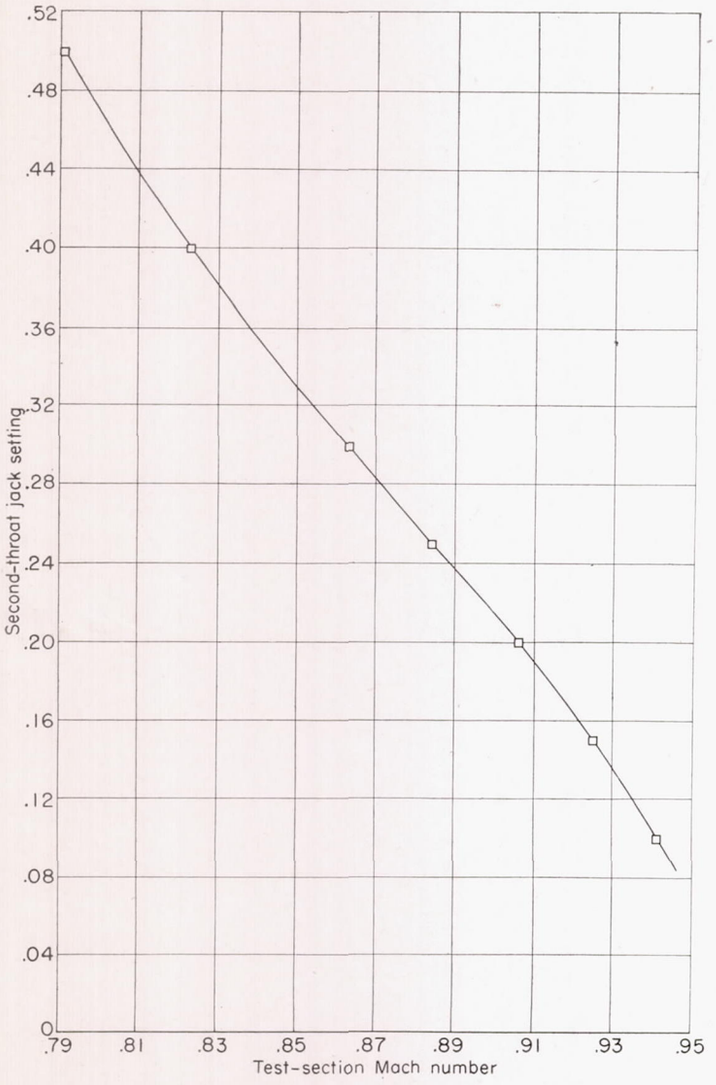

FIGURE 46.—Second-throat calibration for subsonic operation.

CONCLUSION

Uniform shock-free flow with continuous control of Mach number has been achieved together with simplicity of construction and ease of operation. As seen from figure 45, over a considerable portion of the supersonic range of operation only one jack control is needed for changing the flow. The repeatability of flows in the tunnel has proved to be excellent, it being possible to repeat any test-section Mach number to within the accuracy of the measuring instruments.

REFERENCES

1. Ferri, Antonio: Experimental Results with Airfoils Tested in the High-Speed Tunnel at Guidonia. NACA TM 946, 1940.
2. Donaldson, Coleman duP.: Effects of Interaction between Normal Shock and Boundary Layer. NACA CB 4A27, 1944.
3. Ackeret, J., Feldmann, F., and Rott, N.: Investigations of Compression Shocks and Boundary Layers in Gases Moving at High Speed. NACA TM 1113, 1947.
4. Allen, H. Julian, Heaslet, Max. A., and Nitzberg, Gerald E.: The Interaction of Boundary Layer and Compression Shock and Its Effect upon Airfoil Pressure Distributions. NACA RM A7A02, 1947.
5. Liepmann, Hans Wolfgang: Investigations of the Interaction of Boundary Layer and Shock Waves in Transonic Flow. Tech. Rep. No. 5668, Air Materiel Command, U. S. Air Force, Feb. 1948; also, The Interaction between Boundary Layer and Shock Waves in Transonic Flow. Jour. Aero. Sci., vol. 13, no. 12, Dec. 1946, pp. 623–637.
6. Liepmann, Hans Wolfgang, Ashkenas, Harry, and Cole, Julian D.: Experiments in Transonic Flow. Tech. Rep. No. 5667, Air Materiel Command, U. S. Air Force, Feb. 1948.
7. Liepmann, H. W.: Boundary-Layer Shock-Wave Interaction. Symposium on Experimental Compressible Flow, Rep. No. 1133, Naval Ord. Lab., June 29, 1949, pp. 39–66.
8. Oswatitsch, K., and Wieghardt, K.: Theoretical Analysis of Stationary Potential Flows and Boundary Layers at High Speed. NACA TM 1189, 1948.
9. Lees, Lester: Interaction between the Laminar Boundary Layer over a Plane Surface and an Incident Oblique Shock Wave. Rep. No. 143, Contract N6ori–270, Task Order No. 6, Office of Naval Res., Contract NOrd–7920, Task No. PRN–2–E, Bur. Ord., U. S. Navy, and Aero. Eng. Lab., Princeton Univ., Jan. 24, 1949.
10. Lagerstrom, Paco A., Cole Julian D., and Trilling, Leon: Problems in the Theory of Viscous Compressible Fluids. Contract N6onr–244, Task Order VII, Office of Naval Res. and Guggenheim Aero. Lab., C. I. T., March 1949.
11. Fage, A., and Sargent, R. F.: Shock Wave and Boundary Layer Phenomena near a Flat Surface. Proc. Roy. Soc. (London), ser. A, vol. 190, no. 1020, June 17, 1947, pp. 1–20.
12. Marble, F.: The Reflection of a Weak Shock from a Supersonic Shear Layer. Sec. III of Problems on Shock Reflection, GALCIT Transonic Research Group, Contract No. W33–038ac–1717(11592), U. S. Army Air Forces, July 1948.
13. Tsien, Hsue-Shen, and Finston, Morton: Interaction between Parallel Streams of Subsonic and Supersonic Velocities. Jour. Aero. Sci., vol. 16, no. 9, Sept. 1949, pp. 515–528.
14. Howarth, L.: The Propagation of Steady Disturbances in a Supersonic Stream Bounded on One Side by a Parallel Subsonic Stream. Proc. Cambridge Phil. Soc., vol. 44, pt. 3, July 1947, pp. 380–390.
15. Lighthill, M. J.: The Position of the Shock-Wave in Certain Aerodynamic Problems. Quart. Jour. Mech. and Appl. Math., vol. I, pt. 3, Sept. 1948, pp. 309–318.
16. Courant, R., and Friedrichs, K. O.: Supersonic Flow and Shock Waves. Interscience Publishers, Inc. (New York), 1948.
17. Preston, J. H.: Visualisation of Boundary Layer Flow. R. & M. No. 2267, British A. R. C., Nov. 1946.
18. Charters, Alex C., Jr.: Transition between Laminar and Turbulent Flow by Transverse Contamination. NACA TN 891, 1943.
19. Dhawan, S.: On the Design and Use of a Flexible Nozzle for the GALCIT 4″ X 10″ Transonic Tunnel. Engineer's Degree Thesis, C. I. T., June 1949.
20. Liepmann, Hans Wolfgang, and Ashkenas, Harry: Shock-Wave Oscillations in Wind Tunnels. Jour. Aero. Sci., vol. 14, no. 5, May 1947, pp. 295–302.

U. S. GOVERNMENT PRINTING OFFICE: 1953